# EFFECTIVENESS OF TTX IN PROMOTING ANATOMICAL RECOVERY FROM MD IN KITTENS

by

Paige A. Northrup

Submitted in partial fulfilment of the requirements for
the degree of Master of Science

at

Dalhousie University
Halifax, Nova Scotia
July 2017

# DEDICATION PAGE

First, I dedicate this thesis to my mother who has always given me unwavering support. Second, to my father who has always taught me to be humble in my abilities. Third, to the blossoms, for without them this thesis and many others would not have come to fruition.

## TABLE OF CONTENTS

## LIST OF TABLES

## LIST OF FIGURES

## ABSTRACT

Monocular deprivation (MD) during the critical period of visual development precipitates neuronal alterations in the dorsal lateral geniculate nucleus (dLGN) of kittens that include significant reduction in axon terminals and dendritic fields reflected by decreased neuron soma size within deprived layers. This thesis examined the effectiveness of binocular retinal inactivation to promote balanced anatomical recovery within eye-specific layers of the dLGN. After 7-days of MD, animals were intravitreally injected with tetrodotoxin (TTX) to abolish retinal activity. Neuron soma sizes were measured across increasing durations of binocular inactivation that extended to 10-days. The reduction in deprived neuron size produced by 7-days of MD was erased following 10-days of binocular inactivation. Although overall size of neurons was slightly reduced following retinal inactivation, balanced neuron size between eye-specific layers was restored to normal. Finally, neurons were considerably larger than those from animals subjected to the same period of monocular inactivation, indicating true recovery.

## LIST OF ABBREVIATIONS USED

BDNF: brain-derived neurotrophic factor

BE: binocular exposure

BLS: binocular lid suture

BV: binocular vision

CCAC: Canadian Council on Animal Care

DD: delayed darkness

dLGN: dorsal lateral geniculate nucleus

DMCM: methyl-6,7-dimethoxy-4-ethyl-β-carboline

ECM: extracellular matrix

GABA: gamma-aminobutyric acid

GAD: glutamic acid decarboxylase

ID: immediate darkness

IF: intermediate filament

LTD: long-term depression

LTP: long-term potentiation

MD: monocular deprivation

NF-H: neurofilament – heavy

NF-L: neurofilament – light

NF-M: neurofilament – medium

NMDA: N-methyl-D-aspartate

NR1: NMDA receptor subunit 1

NR2A: NMDA receptor subunit 2-A

NR2B: NMDA receptor subunit 2-B

NR2C: NMDA receptor subunit 2-C

NR2D: NMDA receptor subunit 2-D

NT-4/5: neurotrophic factor 4; neurotrophic factor 5

OD: ocular dominance

P: post-natal

PBS: phosphate buffered saline

PHA-L: phaseolus lectin

PNNS: perineuronal nets

RO: reverse occlusion

SMI-32: monoclonal antibody to non-phosphorylated NF-H

TTX: Tetrodotoxin

UCLA: University Committee for Laboratory Animals

V1: primary visual cortex

## ACKNOWLEDGMENTS

Foremost, I would like to express my sincere gratitude to my advisor Dr. Kevin Duffy for continuous support of my MSc thesis. For his patience, motivation, enthusiasm, and immense knowledge. Finally, for inspiring me to further my education and pursue this MSc degree.

Besides my advisor, I would like to thank the rest of my thesis committee: Dr. Donald Mitchell and Dr. Steven Barnes. To Dr. Mitchell, thank you for all the wisdom you have shared with me while working in your lab, and after as a graduate student. I am so grateful for the opportunities you extended to me. To Dr. Barnes, thank you for having faith in my abilities and the opportunity to learn from you.

Last but not least, I would like to thank to my family: to my mother Carol, for your support throughout this process; and to my dad Curtis and my mama D for always telling me I could do big and better things.

# CHAPTER 1: INTRODUCTION

Neuroplasticity refers to the capacity of the brain to rewire or modify neural connections often in response to changes in the environment. Synaptic plasticity exists in different forms across both the juvenile and adult brain and therefore has a diverse range of types and functions (Nys et al. 2015). If the mechanisms that underlie anatomical and behavioural plasticity in the visual system can be understood, further investigation in this area could elucidate those mechanisms involved in, for instance, learning and memory as well as overall sensory processing (Rauschecker 1991). For example, a commonly studied form of synaptic plasticity called long-term potentiation (LTP) occurs in the brain by way of correlated pre- and postsynaptic activity (Bliss and Lømo 1973). Cooke and Bear (2010) demonstrated that LTP and synaptic plasticity are experience dependent in the primary visual cortex of mice. Furthermore, studies have linked the development of LTP with learning and memory in the hippocampus (Teyler & Fountain 1987; Fonseca et al. 2004). Whitlock et al. (2006) conducted a study on inhibitory avoidance learning in rats and concluded that such learning can induce LTP. Therefore studying synaptic plasticity is pivotal for proper interpretation of many aspects of neural development as well as how experience shapes it.

A brief overview of the visual pathway of the cat is useful for this thesis. In the cat visual system, the retina projects to many different structures one of which is the dorsal lateral geniculate nucleus (dLGN), a relay center embedded in the thalamus is the principal target (Chalupa & Williams 1984). The dLGN comprises 3 superficial layers

that are apparent in Nisl stained sections: layer A, layer A1 and layer C. The most recognizable and studied layers of the dLGN are the most superficial ones that are divided into layers A and A1. Each layer receives input from either the ipsilateral or contralateral eye, and is therefore monocular. These layers are stacked in a retinotopic manner, so a perpendicular line through them represents the same territory in visual space (Sanderson 1971). Within these layers there are also different classes of relay cells that are called X- and Y-cells (LeVay & Ferster 1977). Relay cells within the dLGN project primarily to layer IV of the primary visual cortex, or area 17, and to a slightly lesser extent to area 18 (LeVay et al. 1978). The pathway from the retina via the dLGN to visual cortical areas 17 and 18 is referred to as the geniculo-cortical pathway (LeVay et al. 1978).

In this thesis, visual system plasticity refers to the strengthening and weakening of synaptic connections within the dLGN and visual cortex during the critical period. Manipulating visual experience by way of monocular deprivation (MD) causes a shift in ocular dominance towards the non-deprived eye (Hubel & Wiesel 1963; Wiesel & Hubel 1963a). Both cats and monkeys have been shown to exhibit experience dependent synaptic plasticity in the visual cortex (Hubel & Wiesel 1963; Headon & Powell 1973). Pioneering studies began in 1959 by Hubel and Wiesel and provided a clear picture of the complex neuroanatomical organization of the cat striate cortex by way of single unit recordings (Wiesel & Hubel 1963b). Various patterns of light stimuli were used to record responses of individual cells at distinct levels within the cortex. From this they were able to elucidate receptive field characteristics of neurons including their orientation selectivity. Hubel and Wiesel (1959) described neuron receptive fields as being either excitatory or inhibitory and, based on arrangement, that they required a specific form,

size, position and orientation of a light stimulus to be activated. Moreover, these recordings eventually led to mapping of monocular as well as binocular cells within the striate cortex (Hubel & Wiesel 1963).

Hubel and Wiesel went on to study characteristics of visual receptive fields such as orientation selectivity, receptive field complexity and diversity of receptive fields within the visual cortex. In 1962 they demonstrated that receptive fields of cells within the striate cortex were more elaborate than the simple on/off concentric receptive fields typical of the dLGN, describing them as having properties they referred to as simple and complex orientations. Simple receptive fields, like retinal ganglion cells and dLGN cells, exhibit distinct excitatory and inhibitory regions in response to small spots of light. Illumination of all or a portion of the excitatory region of a cell with a simple receptive field would increase firing rate of that cell. Complex receptive fields however were typically larger, more intricate and exhibited more elaborate properties than simple receptive fields. Cells with complex receptive fields responded poorly or not at all to small spots of light shone on their receptive fields but instead to various stationary forms as well as moving shapes but their maps could not be predicted on the basis of their responses to small spots of light (Hubel and Wiesel 1962). Cells of similar receptive field orientation were found to be located next to one another, therefore the cortex was described as being divisible into columns of neurons that exhibited similar receptive field orientation selectivity (Hubel and Wiesel 1962). These columns were deemed orientation columns (Hubel and Wiesel 1962). Following these studies, Shatz and Stryker (1978) shed light on, what are now known as, ocular dominance columns. Ocular dominance columns were analyzed in their 1978 paper when the pair used radioactive labeling to

illuminate the anatomical distribution of geniculocortical afferents serving both eyes within the striate cortex. From this study they determined that the patches, or columns, within layer IV of the striate cortex serving the deprived eye were smaller, and those serving the non-deprived eye were larger than normal. Although these studies were pivotal in understanding the functional architecture of visual pathways in the cat brain, a complete understanding of what function these columnar organizations serve has been elusive.

Next, Hubel and Wiesel (1963a) aimed to understand the differences between the kitten and cat visual pathways and how early visual experience shape the development of neural networks. With this they determined that visual experience is not necessary for proper development of dLGN receptive fields in kittens. Ocular dominance columns as well as orientation selectivity of some receptive fields were also present in the visual cortex of very young kittens (Hubel & Wiesel 1963a). Therefore early visual experience appeared not to be required for the formation of neural connections that govern these aspects of visual system development. From here they went on to reveal the extent to which visual experience, or lack there of, could influence the development of visual pathways. Newborn kittens were subjected to monocular deprivation by way of one eyelid being sutured shut for 3 months (Wiesel & Hubel 1963a). In examination of the dLGN, all animals exhibited profound atrophy within the geniculate layers receiving input from the deprived eye. Neuron somata decreased by an average of 40%; there was also a reduction in overall synaptic activity of neurons in the deprived layers. Newborn kittens that were allowed normal patterned vision naturally had smaller geniculate cells than an adult cat, these cells were even smaller in the atrophic layers of kittens who were

deprived (Wiesel & Hubel 1963a). Subsequent single cell recordings were taken to determine the effects of monocular deprivation on visual development in newborn kittens (Wiesel & Hubel 1963b). Deprivation began at birth and lasted 2-3 months; measured behaviourally, these animals were unable to detect form, and their visual placing abilities were nonexistent. Physiological recordings from the striate cortex revealed that the non-deprived eye, which had normal receptive field characteristics, drove the majority of cells. The deprived eye, on the other hand, could influence very few neurons, of which most had abnormal receptive fields (Wiesel & Hubel 1963b). Taken together these results suggested that newborn kittens have the capacity to develop completely normal visual pathways without visual experience, however, a dramatic disruption of visual experience early in postnatal life, such as that produced by monocular deprivation, can alter connections already established at birth.

According to Guillery and Stelzner (1970) there were two possibilities for the changes described in the visual pathways of kittens when deprived for 3 months from birth. One is that the lack of growth may be a direct result of deprived vision and therefore not a response to events at the cortical synapse (Hubel & Wiesel 1965). The other is that the lack of growth may be because axons of deprived neurons are unable to compete with axons of non-deprived neurons. Guillery and Stelzner (1970) describe a large binocular segment in the dLGN where non-deprived neurons project axons into parts of V1 that overlap with axons from deprived dLGN neurons. They postulated that if the lack of growth that occurs in the deprived layers were due to deprivation and not due to cortical competition, the growth would be equally affected in all parts of the deprived layer. However, if cortical competition were responsible for the lack of growth then the

binocular cells within the deprived layers would be more affected, as the monocular cells have no competition. To test this they sutured the right eye of 3 kittens for between 80 and 90 days, with deprivation begun at postnatal day 7. In each dLGN they saw that the monocular segments were not influenced by deprivation; however, large MD effects were found in the binocular segments. This is exactly what they expected if cortical competition were responsible for the effect of deprivation in the dLGN (Guillery and Stelzner 1970). Following these results, Guillery then tested the influence of binocular lid closure to determine its effectiveness compared to monocular lid sutures. He found that bilateral lid suture had little or no affect on the growth of neurons in the dLGN, which appeared normal. These results further support the idea of binocular competition as an explanation for decreased cell size within deprived-eye layers of the in the dLGN following MD (Guillery 1973).

To delineate the period of sensitivity to monocular deprivation, Hubel and Wiesel (1970) monocularly deprived kittens of visual experience for different durations at various ages to determine the critical period for visual vulnerability to the effects of monocular deprivation. So-called critical periods of development are found in many developmental systems that promote changes in anatomy and behavior (Rauschecker 1991). Physiological recordings from the striate cortex revealed that kittens are most vulnerable to the effects of deprivation during the $4^{th}$ postnatal week (Hubel & Wiesel 1970). This vulnerability remains high until the $6^{th}$ to $8^{th}$ postnatal weeks when it declines to no effect during about the third month of life (Hubel & Wiesel 1970). During this period of heightened sensitivity, monocular deprivation for as little as 3 days can lead to a decrease in the number of cells driven by the deprived eye. Moreover, a 6-day monocular

deprivation period produced results similar to those of kittens deprived for 3 months. The deprived eye could influence only 7% of neurons in the striate cortex and neuron somata within deprived layers of the dLGN were significantly smaller than those in the non-deprived layers (Hubel & Wiesel 1970). Animals that received a deprivation of 6 to 9 days exhibited a near complete shift in ocular dominance from the deprived eye to the non-deprived eye in the visual cortex (Hubel & Wiesel 1970). As mentioned previously, Shatz and Stryker (1978) also saw an ocular dominance shift among cortical cells in layer IV of the primary visual cortex of cats. Following an early period of monocular deprivation they injected a radioactive label into one eye while simultaneously recording from neurons in layer IV. In normal cats, neurons of layer IV in the visual cortex were grouped according to eye preference. In deprived cats the groups of neurons influenced by the deprived eye were smaller than those of normal animals while those influenced by the non-deprived eye were larger. Moreover, the radioactive label enabled visualization of afferents and locations of neurons in layer IV of the visual cortex, which were dominated by the injected eye. This revealed a clear ocular dominance shift as a result of monocular deprivation (Shatz and Stryker 1978). Taken together, this provided evidence that neural connections from the dLGN to the primary visual cortex were being disrupted and modified to adapt to the changes caused by monocular deprivation during the critical period for visual vulnerability.

The adult cat is not vulnerable to the effects of monocular deprivation due to closure of the critical period (Hubel & Wiesel 1970). Even under extreme deprivation conditions, when the period of deprivation is prolonged to 3 months, in adult cat neurons of the visual cortex retain their ability to be driven by the deprived eye (Hubel & Wiesel

1970). As previously mentioned, Hubel and Wiesel (1970) estimated the critical period of visual vulnerability to peak at 4 postnatal weeks of age. In 1980 Olson and Freeman subjected 13 kittens to monocular deprivation at ages spaced regularly through the first 4 postnatal months of life in an attempt to refine the onset of the critical period. Each kitten was subjected to 10-12 days of monocular deprivation; at the end of each animal's deprivation period ocular dominance was measured in the striate cortex using single-unit recordings. From this they determined that susceptibility to monocular deprivation rose until postnatal day 28 and remained at peak vulnerability until postnatal day 48. The effects of monocular deprivation then decreased gradually to the end of the 4$^{th}$ postnatal month. In their research Olson and Freeman aimed to define the exact time course of visual cortical vulnerability to enable further understanding of the mechanisms that underlie the effects of monocular deprivation and plasticity of the visual pathways (Olson & Freeman 1980). Cynader and Mitchell (1980) shed further light on the critical period for visual vulnerability when they subjected newborn kittens to a 4-month period of normal vision followed by monocular deprivation for 3 months. Modification of binocular cortical connections was present even in these animals, although less pronounced, indicating that the critical period for vulnerability to the effects of monocular deprivation extended to between 5 and 8 months (Cynader & Mitchell 1980). Simultaneous studies were completed on kittens' dark reared for 4, 6, 8 and 10 months prior to monocular deprivation. All dark reared animals exhibited an ocular dominance shift in the visual cortex from the deprived eye to non-deprived eye. Data from these studies indicate that the critical period for visual vulnerability not only depends on age but also on the visual experience the animal is subjected to in early postnatal life (Cynader & Mitchell 1980). Furthermore, in 1985 Mower and Christen reared cats in complete darkness from birth to

4-5 months of age, with this they found that the majority of visual cortical cells were binocularly driven and overall ocular dominance was not different from that of normal cats. These results indicate that balance of visual experience is crucial to development, while quality of visual experience is not. Mower and Christen (1985) also found that a period of MD imposed after dark rearing concluded in an ocular dominance shift towards the dominant eye. These findings suggest that balanced visual input plays a role in activating the underlying plasticity mechanism in the cat visual cortex and that dark rearing can delay these processes therefore susceptibility to MD is prolonged (Mower & Christen 1985). Finally, Daw et al. (1992) deprived 8-9 and 11-12 months old cats for 3 months. These studies provided evidence for critical period closure, in that the critical period for visual vulnerability to the effects of monocular deprivation terminates at about 8-9 months of age (Daw et al. 1992).

Specific anatomical modifications to neural circuitry as a result of monocular deprivation, such as a reduction in neuron somata size in deprived layers of the dLGN (Wiesel & Hubel 1963a) and ocular dominance shifts in the primary visual cortex (Hubel & Wiesel 1970; Shatz and Stryker 1978), were crucial to understand in order to uncover the mechanisms underlying such anatomical changes. Antonini and Stryker (1993) studied the processes underlying the anatomical changes in the dLGN using the radioactive tracer phaseolus lectin (PHA-L). The tracer was injected into the left and right layer A of the dLGN in short term and long term deprived kittens. From this research they could examine the left and right hemispheres of the same animals to visualize the anatomical changes in the deprived layers. In examining the results they saw that afferents serving the deprived eye showed a reduction in complexity of arborization and

afferents serving the non-deprived eye expanded. Later, in 1996, the same group set out to study the process underlying ocular dominance shifts using transneuronal transport of a radioactive label, which was injected into the vitreous humour of one eye to reveal the pattern of innervation from the dLGN in layer IV of the primary visual cortex. In the primary visual cortex of animals allowed to develop normally layer IV is divided into ocular dominance columns, which serve the ipsilateral or contralateral eye, and these columns alternate every 1 mm (Antonini & Stryker 1996). Six to seven days of monocular deprivation in kittens at the 4-5$^{th}$ postnatal week was sufficient to induce shrinkage of the afferents and therefore the territory in layer IV influenced by the deprived eye. In this study geniculocortical afferents were anatomically divided into X and Y cells as discussed above. The duo concluded that both short-term and long-term deprivation most severely affected Y-cells. Shrinkage of these neurons was described as a loss of density and complexity by way of reduced axonal membrane as well as a reduction in branching. Moreover, shrinkage appeared to be due to the reduction or elimination of branches that had developed prior to monocular deprivation (Antonini & Stryker 1996). These results are in concordance with Mower et al. (1981) who found that the process of MD disturbs differentiation of cell types into X and Y geniculate cells. Moreover the processes by which X-cells enable the ability to resolve high spatial frequencies were also disturbed with MD (Mower et al. 1981). Finally, in a later study it was determined that binocular deprivation does not cause the same anatomical changes as monocular deprivation does. Neuronal arborization was indistinguishable from normal, further supporting the idea that normal development occurs without visual experience and it is the disruption of this experience that causes loss of circuitry (Antonini & Stryker 1998).

Understanding the neural mechanisms underlying critical periods of development could help neuroscience transfer the heightened capacity for learning during these periods in the adolescent brain into adulthood (Hensch 2005). Afferents from the dLGN innervate layer IV of the primary visual cortex to produce alternating ocular dominance columns, as mentioned above. Long-range lateral inhibition in the visual cortex provides a scaffold for competing inputs from the left and right eye to layer IV. The balance between excitatory and inhibitory inputs in the visual cortex is susceptible to change; therefore disrupting activity pharmacologically with agents such as diazepam or total silencing of activity via Tetrodotoxin (TTX) will disrupt plasticity (Hensch 2005). ϒ-aminobutyric acid (GABA) is the primary inhibitory neurotransmitter and is synthesized by two isoforms of glutamic acid decarboxylase (GAD), GAD67 and GAD65 (Hensch et al. 1998). GAD67 is found throughout the cell whereas GAD65 is located in the axon terminal and synaptic vesicles. Inhibitory interactions via GABA are known to play a vital role in visual cortical plasticity; this is supported by pharmacologically manipulating $GABA_A$ receptors during a period of monocular deprivation. $GABA_A$ agonists can produce a shift in in ocular dominance to the deprived eye that opposes the normal shift produced by deprivation towards the non-deprived eye (Hensch et al. 1998). Transgenic mouse models provide evidence for the role of endogenous GABA in visual cortical plasticity. Knockout mice for the smaller isoform GAD65 have reduced intrinsic inhibitory transmission. Moreover, biochemical analysis provides evidence that GAD65 contributes a greater amount to total GABA concentrations during early postnatal life in the mouse than the larger isoform GAD67 (Hensch et al. 1998). In 1998, Hensch et al. used transgenic knockout mice for GAD65 to illuminate the role GABA plays in visual cortical plasticity. They found that knockout mice for GAD65 had greater activation to visual stimuli in the visual cortex,

and in fact exhibited hypersensitivity to visual stimulation after a period of dark rearing. Moreover, after a 4-day period of monocular deprivation the knockout mice exhibited no shift in preference to the non-deprived eye. Following this, Hensch et al. (1998) rescued the seemingly lost visual cortical plasticity using diazepam, inducing a complete ocular dominance shift in favour of the non-deprived eye. Taken together these results show that inhibitory input via $GABA_A$ receptors is necessary for visual cortical plasticity between competing eyes during monocular deprivation. Excitatory input is also important to balance inhibitory input within the visual cortex (Hensch and Stryker 2004). Excitatory connections extend afferents from the dLGN over certain areas. Inhibitory connections do not extend afferents as far as excitatory connections do and therefore this balance modulates the shape of connections within the visual cortex. Thus, ocular dominance columns are either broadened or narrowed by excitatory or inhibitory connections in the visual cortex based on neuronal activity (Hensch and Stryker 2004). Hensch and Stryker (2004) tested the broadening and narrowing of columns in the visual cortex of developing kittens. They measured the final size of ocular dominance columns after altering intrinsic GABA inhibition via diazepam infusions into the visual cortex for 1 month beginning 2 weeks postnatal. Diazepam is a GABA agonist, after chronic infusion, Hensch and Stryker saw reduced binocularity in ocular dominance, moreover columns near the infusion site of diazepam were wider than those surrounding them. Following this they did the reverse by infusing an inverse agonist, methyl-6,7-dimethoxy-4-ethyl-β-carboline (DMCM). From this they found that columns in front of the infusion site were narrower than columns surrounding them. These results support the hypothesis that the inhibitory control of endogenous GABA contributes to ocular dominance between input from the left and right eyes to the visual cortex, and therefore visual cortical plasticity (Hensch and

Stryker 2004). The critical period for visual vulnerability can also be induced early by overexpressing brain derived neurotrophic factor (BDNF) to accelerate the maturation of GABA neurons (Hensch 2005). The relationship between BDNF and GABA helps to explain the effects of dark rearing or dark exposure as well. Placing an animal in the dark for a period of time reduces BDNF levels as well as GABA transmission in the visual cortex therefore delaying the onset of the critical period (Hensch 2005). Studies have also shown that the onset of the critical period for visual vulnerability coincides with the emergence of paravalbumin-positive cells, which are accelerated by BDNF overexpression (Huang et al. 1999). $GABA_A$ receptors are localized to receive paravalbumin-positive synapses that are gradually wrapped in perineuronal nets (PNNS) of extracellular matrix (ECM) molecules with age (Härtig et al. 1999). This is thought to mediate the inhibitory effects of GABA and therefore reduce visual cortical plasticity with age. When ECM molecules are disrupted ocular dominance shifts can be induced, once again, even into adulthood (Pizzorusso et al. 2002). Disruption of the ECM can be caused by proteolysis, which is increased after 2 days of monocular deprivation. Moreover, a substantial loss of dendritic spines is seen within the visual cortex after only 4 days of monocular deprivation, which helps to explain loss of function presumably due to loss of connections (Mataga et al. 2004).

The N-methyl-D-aspartate (NMDA) glutamate receptor also plays a key role in neuroplasticity (Quinlan et al., 1999a; Quinlan et al., 1999b) NMDA receptors mediate excitatory neurotransmission in the visual cortex, which balances the intrinsic inhibitory neurotransmission via GABA (Chen et al. 2000). In various regions of the brain, NMDA currents are refined throughout development and are thought to determine net calcium

influx as well as critical period onset (Fagiolini et al. 2003). The NMDA receptor is composed of subunits NR1 and NR2 of which five subunits have been cloned; NR1, NR2A, NR2B, NR2C and NR2D (Chen et al. 2000). In the cerebral cortex NR1, NR2A and NR2B are the dominant subunits whose kinetics are activity dependent. In the cat visual cortex, blockade of NMDA receptors during development causes a reduction in ocular dominance shifts elicited by MD (Quinlan et al. 1999a; Quinlan et al. 1999b). In 2000, Chen et al. demonstrated that the NR2A subunit expression was high at the peak of the critical period and declined with the capacity for visual cortical plasticity. Moreover, NR2A expression aligned with the effects of dark rearing on visual cortical plasticity as well, in that dark rearing slowed both the decline in NR2A expression and closure of the critical period. Later studies by Fagiolini et al. (2003) used transgenic mice carrying a disrupted gene for the NR2A subunit to show that the timing of the critical period was in fact not based on NR2A function alone. NMDA receptors balance inhibitory input by promoting circuit rearrangement in the developing visual cortex. Their results suggest that it is the NMDA receptor current duration that promotes ocular dominance shifts in response to monocular deprivation during the critical period. Moreover, prolonged NMDA currents impaired ocular dominance in both normal and transgenic mice by altering the pattern of neural activity. However, ocular dominance plasticity was fully rescued with the use of diazepam (Fagiolini et al. 2003). Alteration of neural activity may be due to calcium influx caused by prolonged NMDA activation. Calcium is an intracellular second messenger that works to activate various kinases and proteases that modulate synaptic plasticity. The process by which kinases and proteases modulate plasticity has been shown to be more effective during the critical period of visual

vulnerability in kittens as opposed to adult cats (Bode-Greuel & Singer 1989; Tsumoto et al. 1987).

In order to understand the mechanisms that underlie increased cell death, reduced dendritic field complexity as well as alteration of neural circuitry that come with monocular deprivation, Bickford et al. (1998) focused on studying the abnormal morphology of dendrites as well as reduced neuron somata in Y-cells of the dLGN. As they describe, the thin and tortuous dendrites of Y-cells in the deprived layers of the dLGN suggest an alteration to the cytoskeleton, therefore their aim was to understand the cytoskeletal changes that come with monocular deprivation (Bickford et al. 1998). Neurofilament is believed to be a major component of the neuronal cytoskeleton and contributes to both structure and function. The neurofilament triplet protein is made up of 3 subunits that are named based on molecular mass. These are neurofilament heavy (NF-H), medium (NF-M), and light (NF-L) (Hoffman & Lasek 1975). Using the antibody SMI-32 that stains the non-phosphorylated form of neurofilament heavy (NF-H), Bickford et al. (1998) examined the dLGN of normal and deprived cats to measure changes in the cytoskeleton. They first discovered that the antibody preferentially stained Y cells in the dLGN, based on morphology and distribution of staining. Their results demonstrated a clear reduction in SMI-32 staining, and therefore non-phosphorylated NF-H, in the deprived layers of the dLGN. It was then concluded that the reduction in staining must be due to cell class competition (Bickford et al. 1998). Taken together these results suggest that changes in Y-cell morphology are due to alterations in the cytoskeleton that manifest as a degradation of NF-H (Bickford et al. 1998; Kutcher & Duffy 2007) and other subunits (Duffy & Slusar 2009).

As mentioned above, neurofilament proteins are neuron specific cytoskeletal components that are essential for the structure of axons and dendrites. NF-H confers a mature state of neurons, and the delayed expression of NF-H is indicative of maturation and stabilization of neuronal networks (Lavenex et al. 2004). In mature neurons, the intermediate-filament (IF) network is composed mostly of neurofilament proteins, which are the most abundant cytoskeletal protein in neurons (Lee et al. 1993). Neurofilament levels have been shown to be stable and low in the developing kitten until P40 at which point they rise to 60% of adult levels by P90 (Duffy & Mitchell 2013; Song et al. 2015). Hensch (2005) has put forth the concept of "molecular brakes" on cortical plasticity, which are molecules that accumulate with development and govern the critical period closure through regulation of plasticity capacity. The temporal profile of the rise of neurofilament expression in the developing kitten therefore suggests neurofilament proteins as potential molecular brakes (Song et al. 2015). Reduced neurofilament reactivity between eye specific layers of the dLGN after monocular deprivation temporally and spatially correlates with change in neuron size (Kutcher & Duffy 2007). In other words, longer deprivation durations produce progressively greater losses of neurofilament reactivity (Kutcher & Duffy 2007). Following this, Duffy and Slusar (2009) demonstrated that a 4-8 day period of deprivation reduced labeling for all three neurofilament proteins within the deprived layers of the dLGN. Quantification of neuron somata size was based on cytoskeletal modification in this study and was found to be parallel with the loss of neurofilament reactivity. This study also put forward the idea of calpain, a calcium dependent protease, as a method for neurofilament reduction via activation of the NMDA receptor and an influx of calcium. This would then catalyze the fragmentation of neurofilament proteins (Duffy & Slusar 2009). Later in 2013, Duffy and

Mitchell examined levels of neurofilament in the visual cortex of kittens that were raised normally until P30 then placed in darkness for either 5, 10 or 15 days. The 10 and 15-day dark reared animals exhibited a significant reduction in neurofilament immunopositive neurons within the visual cortex to about 50% of normal levels, however there was no change in 5-day animals. Moreover, dark exposure induced rapid recovery from the effects of monocular deprivation (Duffy & Mitchell 2013). According to Lee and Shea (2014) phospho-mediated NF-H interactions are thought to provide stability to the axonal cytoskeleton. Phospho-NF-H isoforms are delayed and undergo the slowest transport and turnover.

Later-developing proteins, like NF-H, are the most abundant in neurons and contribute greatly to the stabilization of neural networks as well as the reduction in capacity for cortical plasticity beyond the critical period peak (Song et al. 2015). Due to the temporal profile of NF-H being synthesized at low levels early in development and increase with the age of the organism, manipulation of NF-H would be expected to effectively modulate plasticity (Song et al. 2015). Therefore, reduced NF-H may be effective in enhancing plasticity capacity the dLGN and visual cortex. Following from this logic, extension of the critical period can be achieved with dark-rearing, which is a rearing condition that produces a reduction in NF-H levels in both the dLGN and the visual cortex (Duffy & Mitchell 2013). Neurofilament proteins are recognized as phosphorylation sites by posttranslational kinases, this phosphorylation confers increased stability to the protein as the animal ages (Myers et al. 1987). As phosphorylated NF-H levels increase neuronal structure will become more stable as the animal ages (Song et al. 2015). This is precisely what Song et al. analyzed in 2015; the visual cortex from kittens

and adult cats were examined for NF-H expression. Results of this study found that NF-H expression levels very low at birth and remained stable and low to P47. Levels began to rise quickly at about P60 reaching 50% of adult levels by P101. At P90 levels were considerably higher than P60 and highest in adults (Song et al. 2015). From these results it is can be presumed that NF-H levels govern critical period closure by increasing stability of neurons and preventing plasticity.

Postnatal development of geniculocortical afferents of the visual pathway is experience-dependent, and disruption to normal vision during the critical period for visual vulnerability will alter proper development of neural connections (Wiesel & Hubel 1963a). One option for recovery from the effects of monocular deprivation is to allow normal pattern vision to the deprived eye during the critical period. Two additional therapies used in previous studies are binocular vision (BV), which provides both eyes with normal vision, and reverse occlusion (RO) in which the originally deprived eye is opened and the other is sutured shut. Recovery has been shown to be greater with reverse occlusion in that it produces both behavioural and anatomical recovery (Mitchell et al. 1977; Antonini and Stryker 1998). In 2012 O'Leary et al. examined the temporal changes of NF-H in the dLGN of monocularly deprived kittens with BV, RO and dark rearing. The results demonstrate that both BV and RO promote NF-H recovery, however, dark rearing catalyzed the loss of NF-H labeling indicating a potential therapeutic effect of dark exposure. Their results showed that 8 days of BV and RO promoted recovery of NF-H, and that this recovery occurs at the same rate as neuron somata size recovery. However, animals that were exposed to darkness showed no recovery of NF-H and instead there was a considerable loss of NF-H labeling in the layers driven by the non-

deprived eye, thereby promoting a heightened state of plasticity in the deprived layers via a decrease in NF-H.

Monocular deprivation has been shown to reduce labeling for NF-H in the visual system of cats, monkeys and humans (Bickman et al. 1998; Kutcher & Duffy 2007; Duffy & Livingstone 2005; Duffy et al. 2007). It has been suggested that the effects of deprivation, such as a decrease in neuron somata size, result from cellular competition for territory (Guillery 1973). Recovery from the atrophy of deprived cells and reduction in NF- H levels seen with monocular deprivation requires removal of competition between the two eyes, as it achieved with BV or RO, both rearing strategies that can produce substantial recovery. Dark rearing likewise eliminates the competitive disadvantage of the deprived eye, however it is does so by reducing visually driven activity in both eyes equally. The binocular elimination of visually driven activity through dark rearing may enhance plasticity capacity through a generalized reduction of neurofilaments that typically stabilize neural circuitry and attenuate plasticity. Taken together this means that full anatomical recovery from monocular deprivation appears to requires not only removal of the competitive imbalance between the eyes, but binocular elimination of visually driven activity that catalyzes a reduction of proteins that inhibit plasticity and attenuate or eliminate the capacity for recovery. The recovery of NF-H to normal levels, seen with BV and RO, acts to strengthen and stabilize deprived neuron circuitry, however, this is done in isolation of the fellow eye whose neural circuitry remains stable and thus cooperative/binocular recovery is prevented.

In knowing complete recovery from MD requires a competitive balance between the two eyes as well as reduced NF-H levels, Duffy and Mitchell (2013) highlighted the importance of binocular vision following dark exposure. This study comprised 3 parts to provide evidence that complete darkness early in postnatal life can provoke a heightened state of visual cortical plasticity by reducing neurofilament and produce instability in the maturing neuronal cytoskeleton sufficient to promote recovery (Duffy & Mitchell 2013). In the first part of this study, kittens were provided with normal visual experience until P30, at which point a 10- or 15-day exposure to darkness reduced neurofilament immunolabeling by 50% of normal levels in the visual cortex. The second part of the study also placed kittens in a period of darkness for 10 days, however these animals were subjected to a 7-day period of monocular deprivation prior to dark exposure, from P30-P37. Within the second part of the study, one group comprised 3 kittens that were placed into darkness immediately following MD (immediate darkness kittens, ID). Another group comprised 4 kittens that were subjected to a delayed period of darkness for either 5 or 8 weeks (delayed darkness kittens, DD). Animals in the ID group emerged from dark exposure completely blind. Vision in both eyes improved slowly following dark exposure to normal visual acuity over a period of 7 days. Animals in the DD group did not experience any immediate negative effects to the non-deprived eye from dark exposure, moreover the acuity of the deprived eye improved rapidly to equal values of the non-deprived eye in 5-7 days (Duffy & Mitchell 2013). This study provides evidence that darkness may be used as a potential therapeutic treatment for the effects of monocular deprivation in that it promotes recovery of visual acuity. Moreover, as previously mentioned darkness promotes recovery of cell size while reducing NF-H levels allowing a heightened period of visual cortical plasticity (O'Leary et al. 2012).

Duffy et al. (2016) studied the effect of periods of darkness on the susceptibility to monocular deprivation in both juvenile kittens and adult cats. The results of this study show that dark exposure prior to MD did not enhance susceptibility in adult cats, however, 10 days of dark exposure prior to a 7-day period of MD in juvenile kittens increased susceptibility to deprivation. Juvenile kittens were deprived at 12 weeks of age, therefore deprivation occurred within the critical period but beyond its peak. These juvenile kittens displayed a reduction in neurofilament immunolabeling in the dLGN. From these results it appears that dark exposure can restore a heightened level of plasticity similar to that at the peak of the critical period for visual vulnerability in juvenile kitten (Duffy et al. 2016). This remarkable recovery seen with dark exposure may be attributed to the lack of visually driven activity. In 2014 Duffy et al. tested binocular lid suture (BLS) as a potential method for recovery from the detrimental effects of monocular deprivation. Kittens were raised normally until P30 at which point they were monocularly deprived for 7 days followed by either a 10-day period of BLS or a 10-day period of complete darkness. While both methods support recovery, only complete elimination of visual experience by dark exposure produces recovery of visual acuity in the deprived eye. Dark exposure results in complete elimination of all visual stimulation whereas BLS allows transmission of some light and low spatial frequency information. This low level of transmission can support brightness discrimination and permit cortical neurons to respond to diffuse light passing through the eyelids (Duffy et al. 2014). Therefore it seems that it is the complete absence of visually driven neural activity that is recapitulating the capacity for visual plasticity.

Monocular deprivation is an animal model that mimics many of the effects of a human vision disorder called amblyopia (Mitchell 1988; Weisel & Hubel 1963, 1965). Deprivation amblyopia, referred to here as monocular deprivation, is caused by the occlusion of vision from one eye or both (Hubel & Wiesel 1965). This deficit causes loss of vision, loss of contrast sensitivity, reduction in visual acuity and loss of motion perception (Wong et al. 2012). Amblyopia is the leading cause of unilateral visual impairment in children, affecting about 5% of the population (Mansouri et al. 2013). Moreover, if the impediments to vision that cause amblyopia are not corrected early in life, the primary visual cortex, and other visual areas, will develop abnormally. This in turn will lead to an intractable vision impairment, age-related ocular degeneration and heightened potential for loss of the non-amblyopic eye due to trauma or infection (Mansouri et al. 2013). Mitchell and Duffy (2014) describe the typical treatment of amblyopia as being a two-step process. The first step is to reduce the cause of amblyopia, and the second is to deprive the dominant eye of pattern vision to promote use of the amblyopic eye. Existing treatment methods for amblyopia lead to visual improvement, however, 50% of patients never reach normal visual acuity (Birch 2013). Occlusion or patching therapy has been a common treatment strategy for amblyopic children, however, compliance is a major issue for various reasons such as disliking the hours spent wearing a patch, therefore the success rate is largely dependent on compliance (Wallace et al. 2013). In 2011, Mitchell et al. set out to determine if all visual input is equal by comparing daily periods of monocular and binocular vision against one another. Their results show that short daily periods of binocular exposure (BE) offset longer periods of monocular vision, thereby allowing normal visual development in both eyes. Daily binocular exposure prevented the development of deprivation amblyopia in the deprived

eye; furthermore it allowed normal development of ocular dominance columns for both the deprived and non-deprived eyes. These results demonstrate the inherent preference that the kitten visual system has for binocular vision in that a period of MD extending into the critical period is not adequate in blocking the remedial effects of binocular vision (Mitchell et al. 2011). From this we can postulate that the use of binocular therapies to restore vision to the deprived eye in deprivation amblyopia would be superior to any monocular treatments, such as patching therapy.

Animal models of deprivation-induced amblyopia originated with the seminal studies of Wiesel and Hubel (1963) discussed earlier. Such animal models permit exploration of treatment strategies that would be difficult if not impossible to employ in humans, such as dark exposure or pharmacological treatments. In knowing that complete darkness exhibits a rapid and complete recovery from the effects of monocular deprivation, one could postulate that a pharmacological treatment mimicking the effects of darkness could also yield remarkable recovery from the effects of visual deprivation. One such compound is tetrodotoxin (TTX), which was first discovered in 1909. TTX is an extremely potent neurotoxin found in various tissues of over 20 species of puffer fish. Direct application of TTX causes sodium channels of excitable tissues to shut down. By acting as a ligand, TTX binds to voltage-gated sodium channels preventing the diffusion of sodium into neurons effectively eliminating action potentials (Bane et al. 2014). Single unit recordings from the primary visual cortex of kittens demonstrated that intracortical infusions of TTX completely prevent an ocular dominance shift typical of monocular deprivation. These results indicate that TTX abolishes all activity in the visual cortex thereby preventing plasticity during deprivation (Reiter et al. 1986). Stryker and Harris

(1986) employed intravitreal TTX injections to block retinal ganglion activity from one eye of kittens. Their results support Reiter et al. (1986) in that TTX blocked all ganglion cell activity and further prevented ocular dominance formation. Moreover, unlike any other deprivation methods, such as dark exposure or lid suture, single unit recordings show that TTX application blocked spontaneous retinal activity, along with all other retinal activity (Stryker & Harris 1986). This has been shown in monkeys subjected to intravitreal TTX injections to eliminate all retinal ganglion activity therefore reducing zinc, an activity marker, in ocular dominance columns receiving input from the injected eye (Dyck et al. 2003). Chapman et al. (1986) used monocular intravitreal TTX injections along with subsequent dark exposure to produce an imbalance in spontaneous activity. This suggests that an imbalance in spontaneous activity was enough to produce an ocular dominance shift towards the non-injected eye, even though the animal was reared in total darkness (Chapman et al. 1986). Taken together, it may be that intravitreal TTX injections mimic dark exposure in that retinal activity is abolished, however, it is a more robust deprivation method in that it blocks all activity. Moreover, binocular retinal inactivation by way of intravitreal TTX injections will remove the competitive disadvantage of monocular deprivation. Finally, binocular application of TTX may lead to superior recovery outcomes compared to monocular treatments. In theory this should restore a heightened level of plasticity similar to that of the peak critical period for visual vulnerability. Using TTX, it may be possible to restore plasticity and improve visual acuity in monocularly deprived kittens with 10 or less days of binocular TTX treatment.

In this study, we examined the effectiveness of binocular retinal inactivation to promote balanced anatomical recovery from the deleterious effects of monocular

deprivation within the eye-specific layers of the kitten dLGN. After 7 days of MD animals were intravitreally injected with tetrodotoxin (TTX) to abolish retinal activity. The objective of this thesis is to assess the potential for a pharmacological treatment of monocular deprivation in kittens as an alternative treatment. Furthermore, we aim to reveal if binocular inactivation will promote a true recovery of cell size compared to monocular inactivation. We have devised a novel 2-D mapping approach to analyze the effects of intravitreal TTX in the dLGN. This technique will enable a retinotopic assessment of recovery for all conditions to reveal where deficits from monocular deprivation are localized within the dLGN. Finally, we will assess the effects TTX has on layer II/III of the visual cortex.

# CHAPTER 2: EXPERIMENTAL DESIGN

## 2.1 – Materials and methods

A total of 15 male and female kittens bred and reared in a closed colony at Dalhousie University were used in this study. All procedures described below were approved by the Dalhousie University Committee for Laboratory Animals (UCLA) and followed the Canadian Council on Animal Care (CCAC) Guidelines. Animals were raised in colony rooms with litter boxes, cardboard boxes and toys with ad libitum dry food and water, wet food was provided once per day. Animals were randomly assigned to 3 conditions: normally reared with binocular vision (n=4), a 7-day period of monocular deprivation (MD) at postnatal day 30 (n=2), or a 7-day period of MD at postnatal day 30 immedately followed by intravitreal injections of tetrodotoxin (TTX). Animals assigned to the injected group were given either 10-days of monocular TTX (n=3), 4-days of binocular TTX (n=2), 6-days of binocular TTX (n=1) or 10-days of binocular TTX (n=3) injections. Procedures in common with all experimental animals as well as those unique to monocularly or binocularly injected animals are described below.

## 2.2 – Monocular Deprivation

Animals were weighed and anaesthetized for surgery on postnatal day 30 with gaseous isofluorane (3-5% in oxygen) and body temperature was maintained at 37°C by placing a heating pad beneath the animal during surgery. A subcutaneous Anafen® (Ketoprofen 0.1ml/g) injection was used as an analgesic prior to surgery for each animal. Alcaine sterile ophthalmic solution (1% proparacaine hydrochloride) was used as a local

anesthetic applied topically to the left eye prior to surgery. The upper and lower palpebral conjunctivae were sutured together using Ethicon 6-0 vicryl, at this point a broad spectrum antibiotic ointment (1% Chloromycetin) was applied topically to mitigate infection. The upper and lower eyelids were then sutured together at the lid margins with Ethicon 5-0 silk thereby providing two layers of occlusion from visual experience. Animals were monitored daily for loose sutures throughout the entire deprivation period to ensure deprivation was complete and equal across animals. No animals in this study had any suture repair surgeries throughout their 7-day deprivation period. On postnatal day 37, animals were weighed and sutures were surgically removed under anesthesia. In all cases the left eye was deprived. Two animals were perfused at this point to be used as 7-day deprived controls. Three additional animals were reared normally to be used as controls and were perfused at P47 according to procedures that are described below.

2.3 – Intravitreal Tetrodotoxin (TTX) injections

The animals within the TTX group were anaesthetized for surgery with gaseous isofluorane (3-5% in oxygen) and body temperature was maintained at 37°C. A subcutaneous Anafen® (Ketoprofen 0.1ml/g) injection was used as an analgesic prior to surgery for each animal. Alcaine sterile ophthalmic solution (proparacaine hydrochloride) was used as a local anesthetic applied topically to the left eye after opening. Following left eye opening, experimental animals received either a monocular or binocular injection of 0.5 $\mu$l of Tetrodotoxin (TTX) per 100 g of body weight. TTX (Abcam, MA, USA; ab120054) was diluted with distilled $H_2O$. The upper and lower eyelids and palpebral conjunctivae were pulled back with forceps in order to expose the corneal limbus.

Approximately 1 mm beyond the corneal limbus a puncture hole was made with a sterile $26\frac{3}{8}$ gauge PrecisionGlide™ needle. This puncture was used as the injection site for each surgery thereafter in order to minimize ocular trauma. TTX was loaded into a sterile 10 µl Hamilton Syringe (GASTIGHT ® #1707, Hamilton Company) and the injected volume was adjusted according to each animal's body weight. Injections were performed slowly, over approximately 15 seconds, to ensure no TTX would leak out of the puncture hole. After each injection was complete, Alcaine sterile ophthalmic solution (proparacaine hydrochloride) was applied again to the eye as a freezing agent. In the case of binocularly injected animals this procedure was then performed on the right eye. Finally, animals were taken off isofluorane and allowed to recover in a cat carrier containing a heating pad to maintain a 37°C body temperature.

Injections were completed every 48 hours in the same manner as above. Animals were binocularly injected for 4 (n=2), 6 (n=1) or 10 (n=3) days before perfusion. After every injection, animals were tested for pupillary reflexes by shining light into each injected eye. Animals were also tested for visual-placing reflex after injections to ensure loss of vision. This was done by lowering an animal toward the surface of a lab table, if the animal could see the surface their visual-placing reflex would engage and their legs would extend. When visual stimulation was abolished with TTX this reflex was temporarily lost and the animal would not extend their legs. Visual-placing reflex was tested in monocular animals as well by placing an opaque, hard contact lens in the non-injected eye.

2.4 – Histology

Two days after their last TTX injection animals were anesthetized with isofluorane (5% in oxygen) prior to receiving a lethal dose of sodium pentobarbital (Euthanyl; 150 ml/kg) delivered intraperitoneally. Animals were then perfused transcardially with 250-350 ml phosphate buffered saline (PBS, 0.1M, 4° C, pH 7.4) followed by 250–350 ml of 4% paraformaldehyde. Brain tissue was extracted from the cranium immediately and dissected with a razor blade to reveal the thalamus. The occipital, frontal and temporal lobes were removed from each hemisphere; the remaining tissue contained both left and right lateral geniculate nuclei (LGN), the left and right primary visual cortex (V1) was also dissected. The dissected brain tissue was then cryoprotected in a solution containing 30% sucrose in 0.1M PBS at 4°C.

Tissue containing the dLGN and V1 were embedded in OCT Tissue Freeze (Triangle Biomedical; Durham, NC, USA) and mounted on a freezing microtome (Leica SM2000R; Germany) where 40 μm thick coronal sections were cut. Sections used for Nissl staining were wet-mounted onto glass slides, allowed to dry overnight, dehydrated using a graded dilution series of ethanol and then placed in cresyl violet for 5 minutes. Sections were then differentiated using the ethanol dilution series to optimize staining of perikaryon, cleared in Histo-clear (DiaMed Lab Supplies Inc.; Mississauga, ON, CAN) and coverslipped with permount (Fisher Scientific; Canada).

A subsection of tissue slices were used for immunohistochemistry and were left free floating in PBS and probed for the presence neurofilament-H (NF-H) using the monoclonal SMI-32 antibody (Covance, 1:1000) that targets the non-phosphorylated

version of neurofilament-H. Antibody specificity was verified using immunoblots of cat visual cortex that gave rise to a single band of immunoreactivity at 130kDa, congruent with previously published data on NF-H (Julien and Mushynski 1982; Kaufmann et al. 1984; Georges and Mushynski 1987). Sections were incubated overnight at 4° C in SMI-32, rinsed with PBS and incubated in a biotinylated secondary antibody (Jackson Immunolabs: 115-065-146, 1:1000). Antibody labeling was then made visible using an avidin-biotin complex, Vectastain ABC kit (Vector Laboratories; Burlingame, CA, USA), and 3'3-diaminobenzadine tetrahydrochloride as chromogen. Reacted sections were mounted onto glass slides, dried overnight, dehydrated with ethanol, cleared in Histoclear and coverslipped using permount.

2.5 – Quantification

All quantification was performed blind to each animal's condition. The density of NF-H label was quantified in layers A and A1 of the right and left dLGN by stereologically counting positively labeled neurons within the defined regions of interest using the optical dissector probe from a stereology program (newCAST; VisioPharm, Denmark). The stereology software generated random samples from 50% of layers A and A1 of the left and right dLGN. Positively labeled neurons expressed homogeneous and dark cytoplasm around a weakly labelled nucleus. Neurons were made visible at 600X magnification using a BX51 compound microscope fitted with a high-resolution DP-70 digital camera (Olympus, Markham, Canada).

Cell size measurements were performed under the same conditions as NF-H, however, a nucleator stereology probe was used to estimate neuron soma area

(newCAST; VisioPharm, Denmark). Only cells with a darkly stained cytoplasm and lightly stained nucleus were measured to avoid inclusion of measurements from glial cells. A minimum of 1500 cells were measured per animal. A deprivation metric was then used to make within animal comparisons of the measurements taken from layers A and A1 of the right and left dLGN for cell size and NF-H density.

Deprivation Metric:

$$= \frac{\text{(Non-Deprived A + Non-Deprived A1) – (Deprived A + Deprived A1)}}{\text{(Non-Deprived A + Non-Deprived A1)}} \times 100 \quad (1)$$

All values close to zero for this deprivation metric were evidence of no difference between measurements taken from the deprived and non-deprived layers of the dLGN (Kutcher and Duffy, 2007; Duffy and Slusar, 2009).

The density of NF-H positive cells in V1 was measured by use of the same procedures employed for the left and right dLGNs. Random samples from within V1 were selected by the program and the optical dissector stereology probe was used to count the number of cells reactive to NF-H. Density of NF-H labeling was calculated by the number of neurons counted divided by the mask area ($mm^2$). Only cells with dark cytoplasmic staining and light nuclear staining were counted to avoid including glial cells. The density of labeled neurons was calculated for layers 2/3, 4, 5 and 6 of both left and right V1 by dividing the total number of counted cells by the size of the region sampled.

2.6 – 2D Colour-coded maps

For this thesis we employed a novel method for anatomical quantification of neurons within the left and right dLGN of the cat (Duffy et al., 2016). Two-dimensional colour-coded maps of neuron somata size and NF-H density from the deprived and non-deprived dLGN layer were created to demonstrate the effects of 7-day MD, 7-day MD plus monocular TTX injections and 7-day MD plus binocular TTX injections. Maps were also created for each control animal. Maps of both the left and right dLGNs were generated using the nucleator stereology probe for cell size and the optical dissector probe for NF-H density (newCAST; VisioPharm, Denmark). 100% of both layer A and A1 of the left and right dLGNs were measured. Only cells with a darkly stained cytoplasm and lightly stained nucleus were measured to avoid inclusion of measurements from glial cells. Cells were then mapped according to x/y coordinates; cell size maps are colour-coded according to cell soma area and NF-H according to density.

For cell soma area maps, in each animal ~2000 cells were measured per layer in both the left and right LGN to configure a precise map of neuron somata size. Measurements of cell areas were placed into 11 bins as follows: <50 $\mu m^2$, 50-79 $\mu m^2$, 80-109 $\mu m^2$, 110-139 $\mu m^2$, 140-169 $\mu m^2$, 170-199 $\mu m^2$, 200-229 $\mu m^2$, 230-259 $\mu m^2$, 260-289 $\mu m^2$, 290-319 $\mu m^2$, >320 $\mu m^2$. Bins were then graphed according to x/y coordinates and colour coded using the RGB colour model. Small cells in bins 1-5 are blue wavelengths ranging from 450nm to 464 nm and large cells in bins 7-11 are red ranging from 700nm to 724nm.

Subsequently, for cell density maps, cells were counted according to NF-H labelling per layer in both the left and right dLGN. Measurements of cells densities were then mapped according to x/y coordinates. Finally, deprived layers of both the left and right dLGN were coded as white and non-deprived layers coded as black.

These pictorial representations of the distribution of cell size and the density of cells per layer of the dLGN help visualize the anatomical changes occurring in the dLGN as a consequence of monocular deprivation, as well as remarkable recovery from monocular deprivation. Furthermore, this novel representation of the effects of MD, as well as the effects of TTX post MD, allowed retinotopic assessments for each condition. This permitted identification of cells were atrophied, due to monocular deprivation, within the dLGN to visualize where recovery if recovery was complete.

# CHAPTER 3: RESULTS

## 3.1 – Control experiments

Results from three kittens that were reared normally to P47 were anatomically consistent with previous studies in both the dLGN and V1. Anatomical investigation on normal animals included measurement of NF-H density and neuron somata size in the dLGN, and NF-H density within V1. Control animals were allowed normal patterned binocular vision until P47 after which they were perfused as described above in the Methods section. Upon gross examination of Nissl-stained dLGN sections, perikarya were easily distinguishable against a much lighter background, and no difference in cell size was observed between layers A and A1 of either the left or right dLGN. Mean cell size for C384: deprived = 169 $\mu m^2$, non-deprived = 177 $\mu m^2$; mean cell size for C385: deprived= 158 $\mu m^2$, non-deprived = 153 $\mu m^2$; mean cell size for C386: deprived= 216 $\mu m^2$, non-deprived = 220 $\mu m^2$ (Table 1). Looking ahead to Figure 9A we can see these results expressed in terms of the deprivation metric (1), cells within left eye layers were about the same size as those in right eye layers for C384, C385 and C386 by, respectively, 4%, -2% and 2% (Figure 9A). Statistical comparison using an independent unpaired samples t-test found the average soma areas between deprived and non-deprived layers to be non-significant : $t(14) = 0.158$, $p = 0.877$.

Similar to our observations from Nissl-stained sections, gross observations of sections immunolabeled for NF-H revealed no difference between left eye and non-deprived layers of both the left and right dLGN. Quantification of NF-H positive neuron density in each layer of the dLGN revealed densities for each animal as follows: C384:

deprived= 230 neurons/mm$^2$, non-deprived = 240 neurons/mm$^2$; C385: deprived = 126 neurons/mm$^2$, non-deprived = 129 neurons/mm$^2$; C386: deprived = 154 neurons/mm$^2$, non-deprived = 152 neurons/mm$^2$. Absolute values for each can be found in Table 2. Analysis using a deprivation metric (1) demonstrated negligible changes in NF-H labeling for C384, C385 and C386 of 4%, 1% and -1% respectively (Figure 10). Difference in the densities were assessed statistically with an independent unpaired samples t-test, which revealed a non-significant difference between groups: $t(10) = -0.113$, $p = 0.913$.

The next anatomical investigation was completed in V1 for all control animals; measurements of NF-H densities were taken within layer II/III of V1. According to Trachtenberg et al. (2000) ocular dominance changes in layers II/III are nearly saturated after 1-2 days of MD. This means that a shift in ocular dominance would originate in layer II/III, therefore our analysis of NF-H density in V1 was focused to layer II/III in the expectation that it a dominance shift would be quantifiable. Four additional normally reared animals were added to this condition, as their tissue was available from a previous study (C244 P47 normal, C186 P36 normal, C320 P37 normal, C320 P37 normal). Quantification of NF-H positive neuron density in the left and right layer II/II of V1 revealed densities for each animal as follows: C384: LV1= 103.86 neurons/mm$^2$, RV1= 173.54 neurons/mm$^2$, C386: LV1= 61.01 neurons/mm$^2$, RV1= 101.85 neurons/mm$^2$, C244: LV1= 121.11 neurons/mm$^2$, RV1= 120.52 neurons/mm$^2$, C186: LV1= 61.95 neurons/mm$^2$, RV1= 73.67 neurons/mm$^2$, C320: LV1= 112.74 neurons/mm$^2$, RV1= 128.67 neurons/mm$^2$, C321: LV1= 116.69 neurons/mm$^2$, RV1= 166.93 neurons/mm$^2$. These values served as control measurements for experimental animals, the mask area

within layer II/III of V1 for each animal ranged from 750 000 $\mu m^2$ to 100 000 $\mu m^2$ (Figure 11A).

Finally, for normal animals we produced colour-coded maps created for the original 3 normal animals (Figure 1) that depicted a 2-dimensional map of soma areas within the dLGN. As previously mentioned, red represents large cells and blue represents small cells. The map for C384 neuron somata size and distribution clearly indicated no difference between layers in the dLGN. Homogeneous distribution of large and small cells was clear throughout A and A1 layers on the left and right side. There was also no difference between layers mapped for NF-H labelling (Figure 5). In examining the map for C385 neuron somata size and distribution, intra-animal differences became evident. Cells in the left dLGN were overall larger than those in the counterpart right dLGN, however there was no difference between layers of either the left or the right dLGN, it is conceivable that this is due to natural variability of cell size within the animal. Moreover, there was no difference seen between layers of the dLGN when examining NF-H labelling. Finally, in the map for C386, neuron somata size and distribution, an intra-animal difference was evident in that the right dLGN was denser than the left dLGN. Even with this difference, distribution and cell size was homogeneous across all layers of the dLGN with overall cell sizes simply being large. In this animal there was no difference seen between layers of the dLGN when examining NF-H labelling.

### 3.2 – Monocular deprivation

As controls for our recovery conditions, two kittens were reared normally to P30, and then subjected to a period of monocular deprivation until P37. These animals

exhibited anatomical changes as a result of the prior deprivation. In this group, animals C242 and C243 were allowed normal patterned binocular vision until P30 at which point they had their left eyes surgically closed following procedures previously explained. Upon gross examination of Nissl-stained dLGN sections, a deprivation effect was seen between layer A and A1 of both the left and right dLGN. Mean cell size for C242: deprived = 175 $\mu m^2$, non-deprived = 209 $\mu m^2$. Mean cell size for C243: deprived= 167 $\mu m^2$, non-deprived = 202 $\mu m^2$. Absolute values for each can be found in Table 1. Expressed in terms of the deprivation index (1), cells in deprived layers were, on average, smaller than those in non-deprived layers for C242 and C243 by, respectively, 16% and 17% (Figure 9A). Statistical comparison using an independent unpaired samples t-test found the average soma areas between deprived and non-deprived layers of MD animals to be significant: $t(6) = 0.-4.478$, $p < 0.05$.

Similar to our observations from Nissl-stained sections, gross observations of sections immunolabeled for NF-H revealed a deprivation effect between deprived and non-deprived layers of both the left and right dLGN. Quantifications of NF-H positive neuron density in each layer of the dLGN revealed densities for each animal as follows: C242: deprived= 277 neurons/$mm^2$, non-deprived = 333 neurons/$mm^2$; C243: deprived = 206 neurons/$mm^2$, non-deprived = 281 neurons/$mm^2$. Absolute values for each can be found in Table 2. Further analysis using the deprivation index (1) demonstrated a change in NF-H labeling, in that it was decreased in the deprived layers, for C242 and C243 of 17% and 27% respectively (Figure 10). Differences in the densities measured for these MD animals with an independent unpaired samples t-test revealed a significant difference between monocularly deprived animals and normal animals: $t(2) = -6.241$, $p < 0.05$.

The next anatomical investigation included measurements of NF-H densities taken within layers II/III of V1. Quantifications of NF-H positive neuron density in the left and right layer II/II of V1 revealed densities for each animal as follows: C242: LV1= 139.58 neurons/$mm^2$, RV1= 148.89 neurons/$mm^2$, C243: LV1= 135.5 neurons/$mm^2$, RV1= 150.01 neurons/$mm^2$ (Figure 11B). Differences in the densities measured for these monocularly deprived animals with an independent unpaired samples t-test revealed a significant difference between the left layers II/III, in contrast the right layers II/III revealed a significant difference between normal and MD conditions: Left: $t(13) = 2.37$, $p < 0.05$, Right: $t(14) = 1.05$, $p = 0.31$.

Finally, we analyzed the colour-coded maps created for the two 7-day monocularly deprived animals (Figure 2). In examining the map for C242 there was a clear and striking MD effect in the deprived layers of both the right and left dLGN, however the effect seemed to be greater in the left dLGN. Neuron somata size and distribution clearly indicated differences between layers in the dLGN, in that the non-deprived layers had a more homogenous distribution of cells and contained more large cells. In agreement with the cell size map, the NF-H immunolabeled map (Figure 6) did indicated an MD effect in that the deprived layers had less NF-H immunoreactivity than non-deprived layers. In examining the map for C243 neuron somata size and distribution, intra-animal differences were evident. Cells in the left dLGN were overall larger than those in the counterpart right dLGN, moreover the left dLGN was much more dense. However, there was no difference seen between layers of either the left or the right dLGN. In contrast to the cell size map, the NF-H immunolabeled map did not indicate a

large enough difference in cell density between deprived and non-deprived layers to be seen with mapping.

By observing the 2-dimensional map for soma area and NF-H density generated for MD animals, a retinotopic effect became evident (Figure 2,6). In the 2-D map for soma area, the deprived layers (right A and left A1) of the dLGN exhibit a greater number of blue, or small cells, within the medial binocular segment than in the lateral monocular segment. Moreover, the NF-H map depicted a much greater density of cells within the monocular segment than seen within the medial binocular segment. Taken together, these 2-D maps demonstrate that monocular deprivation affects the medial binocular segment, which is in agreement with previous studies (Guillery & Stelzner, 1970).

3.3 – 7-day MD + 4-day binocular retinal inactivation

In the first recovery experiment, 2 kittens (C367, C370) were reared normally to P30, and then were subjected to a period of monocular deprivation until P37, followed by binocular inactivation with intravitreal TTX for a 4-day period, under conditions described in the Methods section. Upon gross examination of Nissl-stained dLGN sections, recovery was obvious but still a small deprivation effect remained between layer A and A1 of both the left and right dLGN. Mean cell size for C367: deprived = 171 $\mu m^2$, non-deprived = 202 $\mu m^2$. Mean cell size for C370: deprived= 132 $\mu m^2$, non-deprived = 145 $\mu m^2$. Absolute values for each can be found in Table 1. Expressed in terms of the deprivation metric (1), cells in deprived layers were, on average, still smaller than those in non-deprived layers for C367 and C370 by, respectively, 16% and 9% (Figure 9A). Statistical comparison using an independent unpaired samples t-test found the average

soma areas between deprived and non-deprived layers of these recovery animals (C367, C370) to be non-significant: $t(6) = -1.033$, $p = 0.341$, supporting our observation of recovery.

Similar to our findings from Nissl-stained sections, gross observations of sections immunolabeled for NF-H revealed a small deprivation effect between deprived and non-deprived layers of both the left and right dLGN. Quantification of NF-H positive neuron density in each layer of the dLGN revealed densities for each animal as follows: C367: deprived= 174 neurons/$mm^2$, non-deprived = 213 neurons/$mm^2$; C370: deprived = 174 neurons/$mm^2$, non-deprived = 212 neurons/$mm^2$. Absolute values for each can be found in Table 2. Further analysis using the deprivation metric (1) demonstrated a change in NF-H labeling, in that it was decreased in the deprived layers, for C367 and C370 of 18% and 18% respectively (Figure 10). Differences in the densities measured for these recovery animals with an independent unpaired samples t-test revealed a non-significant difference between groups: $t(6) = -2.202$, $p = 0.069$.

Finally, we analyzed the colour-coded maps created for the two 7-day MD + 4-day binocular TTX recovery animals (C367, C370). In examining the cell size map for C367 there was no obvious deprivation effect between deprived and non-deprived layers of either the right or left dLGN. However, the distribution of cells was clearly denser in the left dLGN indicating an intra-animal difference between the left and right dLGN. In agreement with cell size map, the NF-H immunolabeled map did not indicate a difference in cell density between deprived and non-deprived layers. In examining the map for C370 neuron somata size and distribution, there was no clear MD effect between deprived and

non-deprived layers of the left or right dLGN. Neuron somata were overall smaller than normal cells in all layers, therefore this may account for the lack of MD effect seen. In agreement with the neuron somata size map, the NF-H immunolabeled map did not indicate a large enough difference in cell density between deprived and non-deprived layers to be seen with mapping.

3.4 – 7-day MD + 6-day binocular retinal inactivation

In the second recovery experiment, 1 kitten (C380) was reared normally to P30, subjected to a period of monocular deprivation until P37, and finally underwent binocular intravitreal TTX injections for a 6-day period, under conditions described previously. Upon gross examination of Nissl-stained dLGN sections a small deprivation effect was seen between layer A and A1 of both the left and right dLGN. Mean cell size for C380: deprived = 181 $\mu m^2$, non-deprived = 201 $\mu m^2$. Absolute values for each can be found in Table 1. Expressed in terms of the deprivation metric (1), cells in deprived layers were, on average, smaller than those in non-deprived layers for C380 by 10% (Figure 9A). Statistical comparison using an independent unpaired samples t-test found the average soma areas between deprived and non-deprived layers of C380 to be non-significant: $t(2) = -2.434$, $p = 0.135$.

In contrast to our observations from Nissl-stained sections, gross observations of sections immunolabeled for NF-H revealed no deprivation effect between deprived and non-deprived layers of both the left and right dLGN. Quantifications of NF-H positive neuron density in each layer of the dLGN revealed densities for C380 animal as follows: deprived= 249 neurons/$mm^2$, non-deprived = 233 neurons/$mm^2$. Absolute values for each

can be found in Table 2. Further analysis using the deprivation metric (1) demonstrated a –6%, or no change, in NF-H labeling for C380 (Figure 10). Differences in the densities measured for this recovery animal with an independent unpaired samples t-test revealed a non-significant difference: $t(2) = 0.295$, $p = 0.795$.

Finally, we analyzed the colour-coded maps created for C380, the 7-day MD + 6-day binocular TTX recovery animal. In examining the neuron somata size map for C380 there was no obvious deprivation effect between deprived and non-deprived layers of either the right or left dLGN. However, the distribution of cells was slightly denser in the right dLGN. The NF-H immunolabeled map did not indicate a large enough difference in cell density between deprived and non-deprived layers to be seen with mapping.

3.5 – 7-day MD + 10-day binocular retinal inactivation

In the third recovery experiment, 3 kittens (C345, C382 and C398) were reared normally to P30, subjected to a period of monocular deprivation until P37, and then underwent binocular intravitreal TTX injections for a 10-day period, under conditions described previously. Upon gross examination of Nissl stained dLGN sections no deprivation effect was seen between layer A and A1 of either the left or right dLGN. Mean cell size for C345: deprived = 125 $\mu m^2$, non-deprived = 122 $\mu m^2$. Mean cell size for C382: deprived= 159 $\mu m^2$, non-deprived = 152 $\mu m^2$. Mean cell size for C398: deprived= 181 $\mu m^2$, non-deprived = 172 $\mu m^2$. Absolute values for each can be found in Table 1. Expressed in terms of the deprivation metric (1), cells in deprived layers and non-deprived layers were, on average, the same size for C345, C382 and C398 by, respectively, by -2%, -5% and -6% (Figure 9A). Statistical comparison using an

independent unpaired samples t-test found the average soma areas between deprived and non-deprived layers of these recovery animals (345, C382 & C398) to be non-significant: $t(10) = 0.394$, $p = 0.701$.

Similar to our observations from Nissl-stained sections, gross observations of sections immunolabeled for NF-H revealed no deprivation effect between deprived and non-deprived layers of either the left or right dLGN. Quantifications of NF-H positive neuron density in each layer of the dLGN revealed densities for each animal as follows: C345: deprived= 236 neurons/mm$^2$, non-deprived = 253 neurons/mm$^2$; C398: deprived = 213 neurons/mm$^2$, non-deprived = 203 neurons/mm$^2$. Absolute values for each can be found in Table 2. The third animal, C382, could not be immunolabeled for NF-H as the brain was extracted without perfusion for use in a separate experiment. Further analysis using the deprivation metric (1) demonstrated no change in NF-H labeling for C345 and C398 of 7% and -5% respectively (Figure 10). Differences in the densities measured for these recovery animals with an independent unpaired samples t-test revealed a non-significant difference between groups: $t(6) = -0.154$,
$p = 0.882$.

Next, colour-coded maps created for the three 7-day MD + 10-day binocular TTX recovery animals (C345, C382 and C398) were analyzed. In examining the map for C345 there was no deprivation effect between deprived and non-deprived layers of either the right or left dLGN. However, cell sizes were smaller than normal in all layers. The NF-H immunolabeled map did not indicate a difference in cell density between deprived and non-deprived layers (Figure 7). In examining the map for C382, neuron somata size and

distribution, there was no deprivation effect between deprived and non-deprived layers of the left or right dLGN. Neuron somata were smaller than normal in all layers. Moreover, neuron somata sizes were smaller in the right dLGN than in the left dLGN. In examining the map for C398 neuron somata size and distribution, there was no deprivation effect between deprived and non-deprived layers of the left or right dLGN. Neuron somata were smaller than normal in all layers. In congruence with the intra-animal difference seen in C382, neuron somata sizes were smaller in the right dLGN than in the left dLGN. The NF-H immunolabeled map did not indicate a difference in cell density between deprived and non-deprived layers.

By observing the 2-dimensional map for soma area and NF-H density generated for 10-day binocularly injected animals, a retinotopic effect became evident (Figure 3, 7). In the 2-D map for soma area, the deprived layers (right A and left A1) of the dLGN exhibit no difference between the lateral monocular segment and the medial binocular segment. As Guillery and Stelzner (1970) described, MD affects the medial binocular segment substantially more than the lateral monocular segment. In binocularly injected animals soma area and cell distribution is homogeneous, in that they resemble a normal animal. This is further support for decreased competition between cells enabling cooperative growth and promoting recovery. The 2-D map for NF-H also reveals a homogeneous distribution of labeled cells.

Our final anatomical investigation included measurements of NF-H densities taken within cortical layers II/III of the visual cortex. Quantifications of NF-H positive neuron density in the left and right layer II/II of V1 revealed densities for each animal as

follows: C345: LV1= 39.08 neurons/mm$^2$, RV1= 86.86 neurons/mm$^2$, C398: LV1= 103.54 neurons/mm$^2$, RV1= 126.24 neurons/mm$^2$ (Figure 11C). Differences in the densities measured for these recovery animals with an independent unpaired samples t-test revealed a non-significant difference between 7-day MD + 10-day binocular TTX animals and normal animals in layers II/III of V1: Left: $t(13) = -1.45$, $p = 0.86$, Right: $t(14) = -0.95$, $p = 0.36$

3.7 – 7-day MD + 10-day monocular retinal inactivation

In the fourth experiment of this thesis, 3 kittens (C342, C348 and C400) were reared normally to P30, subjected to a period of monocular deprivation until P37, and then underwent monocular intravitreal TTX injections in the left eye for a 10-day period. This condition was necessary to determine if binocular TTX injections would promote a true recovery, or if it would cause a generalized reduction in cell sizes equivalent to the effect of monocular TTX. Upon gross examination of Nissl stained dLGN sections an deprivation effect was seen between layer A and A1 of both the left and right dLGN. Mean cell size for C342: deprived = 96 μm$^2$, non-deprived = 158 μm$^2$. Mean cell size for C348: deprived= 144 μm$^2$, non-deprived = 215 μm$^2$. Mean cell size for C400: deprived= 155 μm$^2$, non-deprived = 244 μm$^2$. Absolute values for each can be found in Table 1. Expressed in terms of the deprivation metric (1), cells in deprived layers and non-deprived layers were the same size for C342, C348 and C400, respectively, by 39%, 33% and 36% (Figure 9A). Statistical comparison using an independent unpaired samples t-test found the average soma areas between deprived and non-deprived layers of these animals (C342, C348 & C3400) to be significant: $t(10) = -3.487$, $p < 0.05$.

In agreement with observations from Nissl-stained sections, gross observations of sections immunolabeled for NF-H revealed a deprivation effect between deprived and non-deprived layers of both the left and right dLGN. Quantifications of NF-H positive neuron density in each layer of the dLGN revealed densities for each animal as follows: C342: deprived= 171 neurons/$mm^2$, non-deprived = 252 neurons/$mm^2$; C400: deprived = 277 neurons/$mm^2$, non-deprived = 280 neurons/$mm^2$. Absolute values for each can be found in Table 2. The third animal, C348, was not perfused therefore its tissue could not be immunolabeled for NF-H. Further analysis using the deprivation metric (1) demonstrated change in NF-H labeling for C342 and C400 of 32% and 27% respectively (Figure 10). Differences in the densities measured for these animals with an independent unpaired samples t-test revealed a significant difference between groups: $t(3) = 10.323$, $p < 0.05$.

Next, the colour-coded maps created for the 3 7-day MD + 10-day monocular TTX recovery animals (C342, C348 and C400) were analyzed. In examining the map for C342 there was a large deprivation effect between deprived and non-deprived layers of both the right and left dLGN. In agreement with the cell size map, the NF-H immunolabeled map indicated a difference in cell density between deprived and non-deprived layers, in that there was less immunolabeling in the deprived layer (Figure 8). In examining the map for C348 neuron somata size and distribution, there was a large deprivation effect between deprived and non-deprived layers of the left and right dLGN. In examining the map for C400 neuron somata size and distribution, there was a large deprivation effect between deprived and non-deprived layers of the left and right dLGN. An intra-animal difference was seen in C400 in that the right dLGN appeared to be

denser. In agreement with the cell size map, the NF-H immunolabeled map indicated a difference in cell density between deprived and non-deprived layers, in that immunolabeling was decreased in the deprived layers.

By observing the 2-dimensional map for soma area and NF-H density generated for 10-day monocularly injected animals, an extreme retinotopic effect became evident (Figure 4,8). In the 2-D map for soma area, the deprived layers (right A and left A1) of the dLGN exhibit a greater number of blue, or small cells, within the medial binocular segment than in the lateral monocular segment. This effect is more extreme than the MD alone and binocular condition. This indicates that monocular TTX does in fact decrease cell size far beyond binocular treatment and supports the true recovery seen with binocular TTX as it exaggerates the competitive disadvantage between the deprived and non-deprived layers. Binocular TTX, in contrast, abolishes the competitive disadvantage between layers and allows cells to grow in conjunction. Moreover, the NF-H map also depicted a much greater density of cells within the monocular segment than seen within the medial binocular segment, again to a more extreme degree than MD alone. Taken together, these 2-D maps demonstrate that monocular TTX affects the medial binocular segment.

The final anatomical investigation included measurements of NF-H densities taken within layers II/III of V1. Quantifications of NF-H positive neuron density in the left and right layer II/II of V1 revealed densities for each animal as follows: C342: LV1= 58.53 neurons/$mm^2$, RV1= 106.37 neurons/$mm^2$, C400: LV1= 134.32 neurons/$mm^2$, RV1= 97.54 neurons/$mm^2$ (Figure 11). Differences in the densities

measured for these animals with an independent unpaired samples t-test revealed a non-significant difference between 7-day MD + 10-day monocular TTX animals and normal animals in layers II/III of V1: Left: $t(13) = -0.14$, $p = 0.89$, Right: $t(14) = -1.19$, $p = 0.25$.

# CHAPTER 4: DISCUSSION

Neuroplasticity exists in different forms across both the juvenile and adult brain and therefore has a diverse range of types and functions (Nys et al. 2015). Visual cortical plasticity allows for investigation of mechanisms required for plasticity at both the anatomical and behavioural level. In this thesis, visual system plasticity refers to the strengthening and weakening of synaptic connections within the dLGN and visual cortex during the critical period. Manipulating visual experience by way of monocular deprivation during this critical period causes a shift in ocular dominance towards the non-deprived eye both in the visual cortex and in the dLGN (Hubel & Wiesel 1963a, 1963b).

It has been well established that the development of geniculocortical afferents of the visual pathway are experience dependent and disruption to normal vision during the critical period alters proper development of neural connections (Wiesel & Hubel 1963a). Moreover, cells in the deprived layers of the dLGN experience anatomical changes in that neuronal soma size are reduced along with an overall reduction in neruofilament levels. An absence of axonal neurofilament proteins prevents axon neurite outgrowth, moreover the loss of neurofilaments has been linked in both space and time with the aforementioned alterations seen in the dLGN and the primary visual cortex (Duffy & Slusar 2009).

According to Guillery and Stelzner (1970) one possibility for shrinkage of cells in the deprived layers of the dLGN of monocularly deprived kittens is that the lack of growth may be because axons of deprived neurons are unable to compete with axons of

non-deprived neurons. Guillery and Stelzner (1970) also detail a large binocular segment where normally innervated cells lie adjacent to deprived cells, this region can be distinguished from the monocular segment of each layer within the dLGN where cells receive input from one eye only. These ideas solidify the notion of binocular competition as an explanation for decreased cell size and decreased neurite growth in deprived layers of the dLGN.

Recovery from the aforementioned anatomical alterations associated with monocular deprivation has been achieved by way of dark rearing or dark exposure following a period of MD (Duffy and Mitchell 2013; Mitchell 2013). Dark exposure eliminates all visually-driven activity, which has been shown to promote recovery of neuronal soma size in deprived laminae and therefore facilitates recovery (Mower et al. 1981). Dark exposure also works to reduce NF, a plasticity brake, thereby preventing structural stabilization (Mitchell & Duffy 2014). The goal of this thesis was to determine if binocular retinal inactivation was capable of recapitulating the plasticity enhancing effects seen with dark exposure.

In this study, we examined the effectiveness of binocular retinal inactivation via intravitreal injection of tetrodotoxin (TTX) to stimulate heightened anatomical plasticity within the kitten dLGN to promote balanced neural recovery from a preceding duration of MD. Results have shown that 10-days of binocular retinal inactivation following MD produces recovery of neuron soma size from the detrimental effects of MD. A novel quantification model by way of 2-D mapping revealed that in binocularly injected animals soma area and cell distribution were balanced between eye-specific layers. Binocular

inactivation reduced cortical competition between the deprived and non-deprived eyes, thereby inducing a balance of NF-H proteins between layers and enabling cells to grow in conjunction. Taken together, our results indicate that balanced elimination of retinal activity is a viable approach to promote recovery from the effects of MD. We speculate that a central mechanism for this recovery involves a lowering of the threshold for synaptic potentiation that enables the weaker deprived eye to regain a level of synaptic strength that is in balance with the fellow eye.

## 4.1 - Normal and MD Animals

When examining the age matched control animals used in this study the results were consistent with previous studies in that their visual system development was undisturbed. No deprivation effect was found in neuron somata size, denoting that neurons were of similar size and distribution throughout the deprived and non-deprived layers of the dLGN. NF-H labeling was also consistent across layers of the dLGN. Furthermore, there were no significant differences in NF-H labeling between layers of the visual cortex. These results indicate that the age matched normal animals developed normally and provided excellent control data.

Animals that underwent a 7-day period of MD were also consistent with previous studies in that the layers of the right and left dLGN that receive input from the deprived eye exhibited smaller neuron soma sizes (Figure 9). The deprivation effect is caused by competitive disadvantage between the cells receiving input from the deprived versus non-deprived eye. This is because decreased neuron somata size indicates decreased dendritic fields, loss of structural proteins and therefore decreased functionality (Hubel & Wiesel

1963a, 1963b; Guillery & Stelzner 1970; Mitchell & Duffy 2014). In accordance with Guillery and Stelzner (1970), our results indicate that a 7-day period of MD affects the medial binocular segment of the dLGN more greatly than the lateral monocular segment. This result indicates that during a 7-day period of MD, cortical competition is responsible for the lack of growth because the binocular cells within the deprived layers were more affected than the monocular cells, as they have little if any competition (Guillery & Stelzner 1970).

Neurofilament results from this thesis were also consistent with previous studies. Labeling for NF-H was lower in deprived layers of the dLGN compared to that of normal animals, moreover the deprivation index for NF-H was significantly different from normal animals (Figure 10). As mentioned previously, Trachtenberg et al. (2000) determined that ocular dominance changes in layers II/III are nearly saturated after only 1-2 days of MD. However, when examining the visual cortex of the MD animals in this study there was no significant difference between MD and normal animals of NF-H labeling in layers II/III (Figure 11). As explained by Trachtenberg et al. (2000) extragranular layers of V1 exhibit a clear OD shift towards the non-deprived eye when electrophysiological responses were measured. Visual pathways in the kitten are not crossed; therefore each V1 received input from both eyes. A random sample within layer II/III of the visual cortex would contain ocular dominance columns for both eyes, therefore if there is a shift and the ocular dominance columns from one eye have shrunk, the overall NF-H densities would actually be lower in and MD animal than a normal animal. Taking into account that NF-H labeling is calculated by its density

(neurons/mm$^2$), the OD shift caused by MD may be obscured when quantifying NF-H, as all cells labeled in layer II/III are included in the calculation.

## 4.2 - Binocular Retinal Inactivation

In the first recovery experiment, 2 kittens (C367, C370) were subjected to a 4-day period of binocular retinal inactivation following MD, while in the second 1 kitten (C380) was subjected to a 6-day period of binocular retinal inactivation following MD. Upon gross examination of the dLGN and V1 sections from these animals a deprivation effect persisted in both cases. While it was clear that a 7-day period of MD was successful in producing a deficit in the deprived eye (Figure 9a), it was evident that a short-term period of binocular retinal inactivation following this MD was not sufficient in producing full anatomical recovery (Figure 9a). Fong et al. (2016) has suggested that this incomplete recovery may be an indication that a short period of binocular inactivation provides a scaffold for visual recovery by priming the visual cortex. A logical question to ask would be if an 8-day period of binocular retinal inactivation would promote full anatomical recovery? Moreover, it may be that an increased dose of TTX would promote anatomical recovery over a short-term period of binocular retinal inactivation following MD, however this would require further investigation due to the toxicity of TTX. If it were true that 8-days of binocular inactivation was capable of promoting full recovery, this would solidify the notion that pharmacologically silencing the retina for 8-days is a quicker and perhaps a more feasible method of recovery than 10-days of dark rearing. These ideas must be tested further in future experiments.

Our third recovery experiment involved 3 kittens (C345, C382 and C398) that were subjected to a 10-day period of binocular retinal inactivation following MD. All three animals in this condition exhibited normal neuron somata sizes in the deprived layers of the dLGN, and the deprivation effect was completely eliminated (Figure 9a). Although the overall size of neurons was slightly reduced following 10-day binocular retinal inactivation, balanced neuron size between eye-specific layers was restored to normal (Figure 9b). Furthermore, neurons were considerably larger than those from animals subjected to the same period of monocular inactivation, indicating a true recovery. Neurofilament quantification for these animals showed no significant difference between 10-day binocular TTX animals and normal animals. This is because the competitive disadvantage was removed between the deprived and non-deprived layers of the dLGN (Figure 10). Our results have further illuminated the need for binocular treatments in promoting absolute recovery from the detrimental effects of MD. Binocular inactivation reduced cortical competition between the deprived and non-deprived eyes. This treatment also promoted a reduction in NF-H levels to allowing cells in the deprived and non-deprived layers to grow synchronously. Taken together, our results indicate that balanced elimination of retinal activity is a viable approach to promote recovery from the effects of MD. We speculate that a central mechanism for this recovery involves a lowering of the threshold for synaptic potentiation that enables the weaker deprived eye to regain a level of synaptic strength that is in balance with the fellow eye.

It is important to this thesis to discuss the affects a 10-day period of binocular retinal inactivation had on the lateral monocular crescent of the dLGN. It is clear that both MD and MD with monocular retinal inactivation severely affected the binocular segment

of the dLGN (Figure 2, 4); however, binocular inactivation following MD did not effect the binocular portion more greatly than it did the monocular segment. This is due to decreased competition within the deprived layers of both the left and right dLGN. During a period of MD many cells lose their connections from the deprived eye in the binocular segment and therefore can only maintain connections from the dominant eye (Wiesel & Hubel 1963), however 10-days of binocular TTX has proven to be effective in promoting a balance between the monocular and binocular segments of the dLGN. Binocular retinal inactivation that accompanies 10-days of TTX reduces the shift of geniculocortical cells to the non-deprived, dominant eye.

Binocular TTX has also revealed that this method of treatment does not decrease neuronal soma size of cells receiving input from the initially deprived eye any further than the original period of MD. This can be seen in Figure 9b; the average neuronal soma size in the deprived eye of binocularly injected animals was not significantly different than that of kittens who underwent and MD only. As stated by Kerr et al. (1972) apoptosis is a result of specific types of cell regression, it is possible that neurons within layers receiving input from binocularly injected eyes of the dLGN will only shrink so far until apoptosis will inevitably occur. This may be why cells do not regress any further with binocular TTX as that would result in cell death within the dLGN. Instead cells in deprived and non-deprived layers regress to a neuronal soma size that would permit them to grow in conjunction. Another explanation may be that cells receiving input from the non-deprived, dominant eye are more susceptible to the effects of TTX due to their larger dendritic fields. Bloomfield (1996) found a direct relationship between the magnitude of reduction in receptive field size of amacrine cells due to TTX injections, and their

dendritic field size. Cells with larger dendritic fields were more susceptible to the effects of TTX in that they experienced a larger reduction in receptive field size. We believe it is reasonable to speculate that this result would hold true for neurons in the dLGN, and that non-deprived cells with larger dendritic fields may be more susceptible to the deleterious effects of TTX. Therefore these cells may experience a greater amount of shrinkage, decreasing neuronal soma size to match that of fellow cells in deprived layers.

According to Kuo and Dringenberg (2009) long-term synaptic depression (LTD) and long-term potentiation (LTP) contribute to anatomical changes that come with experience dependent modifications in the visual system. Periods of darkness as short as 2-5 hours can lower LTP/LTD induction threshold in the rat visual cortex, thereby allowing synaptic strengthening in the retino-geniculo-cortical pathway (Kuo & Dringenberg 2009). This idea is in concordance with Philpot et al. (2007) who discuss the reduction of the NR2A/B subunit ratio of NMDA receptors that coincide with dark rearing which also promotes the reduction of LTP/LTD induction thresholds in that reducing the NR2A/B subunit ratio of NMDA receptors prolongs NMDAR current durations. It is plausible to suggest that binocular retinal inactivation by way of binocular TTX injections reduce the threshold for LTP in kittens by employing the same mechanisms as dark exposure. Dark exposure eliminates all visually driven activity, which enhances the capacity for plasticity and therefore facilitates recovery (Mower et al. 1981). Dark exposure works to reduce NF, a plasticity brake, thereby preventing structural stabilization. Dark exposure has also been found to recover the loss of a growth factor, NT-4/5, following MD thereby preventing further atrophy of deprived neurons (Duffy et al. 2014). Furthermore, dark exposure alters NMDA receptors in that it leads to

a decrease in NR2A/B ratio. This change in NMDARs is expected to lower the activation threshold for LTP, by prolonging NMDR current duration, which is involved in the regulation of neuroplasticity (Philpot et al. 2007). Together, this would permit synaptic strengthening of cells in the deprived layers of the dLGN. Moreover, synapses have been observed to compete for limited "plasticity factors" which can limit the expression of LTP (Fonseca et al. 2004). Binocular inactivation would reduce cortical competition between the deprived and non-deprived eyes; therefore "plasticity factors" would be more readily available to both layers enabling them to grow in conjunction. Together, reduced threshold for LTP, reduced cortical competition and more readily available "plasticity factors" would enable cells within the deprived layers to grow alongside the non-deprived cells and produce a normal balance between inputs from the eyes. These results suggest that binocular retinal inactivation recapitulates the plasticity-enhancing effects of dark exposure by way of restoration of balanced competition between eye-specific inputs that fosters cooperative anatomical development and sets the stage for functional recovery.

### 4.3 - Monocular Retinal Inactivation

Our fourth experiment involved 3 kittens (C342, C348 and C400) that were subjected to a 10-day period of monocular retinal inactivation following MD. This condition was included to rule out any chance of monocular inactivation having an effect on injected cells equivalent to that of binocular inactivation. All results from this portion of the study suggest that monocular retinal inactivation exacerbates the effects of 7-day period of MD in the deprived layers of the dLGN. Furthermore, neurons receiving input from the deprived, injected eye, were considerably smaller than those from animals subjected to the same period of binocular inactivation. In contrast, neurons receiving

input from the non-deprived, non-injected eye, were considerably larger than those from animals subjected to the same period of binocular inactivation (Figure 9b). Monocular TTX caused extreme atrophy of injected cells past the point of binocularly injected animals. Moreover, cells receiving input from the non-injected eye grew larger than normal cells. During early stages of kitten cortical development, spontaneous retinal activity is capable of supporting activity-dependent competition between afferents from the eyes (Greuel et al. 1987). Activity dependent long-term changes of neuronal transmission require that cortical neurons be activated beyond a critical threshold (Greuel et al. 1987). In knowing TTX blocks all retinal activity, including spontaneous activity, it is possible that TTX is effective in producing an exaggerated MD effect when injected monocularly by surpassing this critical threshold. Together our results indicate that binocular TTX enables a balance of cell size between deprived and non-deprived layers of the kitten dLGN, while monocular TTX exaggerates the competitive disadvantage further confirming a true recovery with binocular inactivation.

Neurofilament quantification for these animals shows a significant difference between 10-day monocular TTX animals and normal animals. This is because the competitive advantage was exaggerated between the deprived and non-deprived layers of the dLGN (Figure 10). Our results show that levels of the cytoskeletal protein NF-H in the deprived layers receiving input from the injected eye are reduced, indicating a destabilization of connections within the deprived layers. In contrast, the non-deprived layers receiving input from the non-injected eye had slightly elevated levels of NF-H, indicating a high level of neural circuitry stabilization and therefore a decreased capacity

for synaptic plasticity. Our NF-H results corroborate that monocular inactivation exaggerates the effects of MD.

When analyzing the 2-D colour-coded maps for the 10-day monocular inactivation following MD condition, it is clear that 10-days of monocular retinal inactivation severely affected the binocular segment of the dLGN, appreciably more than an MD alone (Figure 2, 4). This is because, as Guillery and Stelzner (1970) uncovered, cortical competition is responsible for the lack of growth in deprived cells of the binocular segment, however the monocular segment was less affected as the monocular cells had no competition. Monocular retinal inactivation that accompanied 10-days of monocular TTX intensified the ocular dominance shift of cells to the non-deprived, dominant eye, therefore the loss of connections from cells receiving input from the once non-deprived eye was amplified. This then led to an increased deprivation effect within the binocular segment of the dLGN. For the reason that the dominant eye in these kittens was allowed patterned visual experience throughout the experiment, it is plausible to suggest that normal vision in the dominant eye may have contributed to the exacerbated effects of the monocular retinal inactivation, as it would have increased competition between cells of the deprived and non-deprived eye. Cells receiving input from the non-deprived, non-injected eye would have had complete access to any plasticity factors available, and would have out-competed all the deprived cells for cortical space, increasing the deprivation effect within the binocular segment of the dLGN.

Together, these results suggest that monocular retinal inactivation exaggerates the detrimental anatomical effects of monocular deprivation by increasing genioculocortical

competition further than MD alone in the dLGN of kittens. Inputs from the non-deprived and non-injected eye were solidified while connections from the deprived, injected eye were dismantled. Moreover, it is clear that monocular retinal inactivation does not have the same effect on injected cells as binocular inactivation. It can be said that binocular inactivation promoted complete anatomical recovery and promoted congruent growth of deprived and non-deprived cells, while monocular inactivation increased the competitive disadvantage.

### 4.4 - Clinical Relevance

Visual cortical plasticity allows for the investigation of mechanisms required for plasticity at both the anatomical and behavioural level. This thesis aimed to illuminate how binocular and monocular retinal inactivation affected anatomical plasticity in the dLGN and visual cortex of kittens.

As stated by Duffy et al. (2014) there is a growing appreciation for binocular treatments of monocular deprivation. Our results have shown that both MD and MD with monocular retinal inactivation results in smaller somata of neurons receiving input from the deprived eye, in comparison to neurons receiving input from the dominant eye. Conversely, 10-days of binocular retinal inactivation was a sufficient treatment for MD by reducing cortical competition and restoring anatomical balance in the dLGN. As discussed in Duffy et al. (2014) both binocular lid suture and dark rearing of kittens are effective in promoting recovery from MD, however only total darkness can provide complete recovery of visual acuity in the deprived eyes of kittens. It is reasonable to presume that since total darkness is effective in promoting recovery by eliminating visual

experience, TTX would also be effective as it completely silences the retina. This is precisely what our results have shown.

Binocular retinal inactivation by way of intravitreal TTX injections is a feasible treatment for MD, as it does not require extensive dark rearing facilities. Additionally, each injection is fast and efficient with minimal trauma to the animal. The injection site remains the same throughout the experiment to minimize damage to the eye and once the animal has recovered from anesthesia, each are free to behave normally in their colony rooms. Finally, the procedures do not require any micromanipulators and are possible with the help of a single lab technician, making this treatment more feasible.

Treatment of animals with MD via binocular intravitreal TTX does present potential limitations. First and foremost is the risk of toxicity that presents itself whenever using TTX. This can be overcome, as it was in our study, by carefully inserting the needles through the sclera in an area free of visible blood vessels. Moreover, each dose is a microinjection that will metabolize out of the eye in 48 hours, with minimal damage to the eye. A second limitation is that it is possible to inject into the lens of the eye. Finally, it cannot be ruled out that the retina and the subsequent geniculo-cortical pathways are not damaged by injections of TTX.

In future research it will be essential to identify whether higher doses combined with shorter durations of binocular TTX injections are sufficient in promoting anatomical recovery. While higher doses do present higher risks for toxicity, this could shorten the time needed for complete recovery. In this thesis, 10-days was sufficient in promoting

complete recovery from the effects of MD, however with slightly higher doses it is plausible that complete recovery could be manifested in less than 10-days. This will be crucial to a complete understanding of the effects of binocular retinal inactivation. It cannot be ruled out that NF-H was involved in the heightened plasticity of the binocularly injected animals as there were labelling differences between deprived and non-deprived layers, however, further studies will be required to understand these differences. It may be true that binocular TTX is effective in promoting anatomical recovery from MD however it must be tested behaviourally if it is to be considered as a treatment.

Monocular deprivation is an animal model that mimics many of the effects of a human vision disorder called amblyopia (Mitchell 1988; Weisel & Hubel 1963, 1965). Existing treatment methods for amblyopia lead to visual improvement, however, 50% of patients never reach normal visual acuity (Birch 2013). Occlusion or patching therapy has been a common treatment strategy for amblyopic children; however compliance is a major issue (Wallace et al. 2013). It is not unconceivable that a pharmacological treatment for amblyopia may be the future of clinical therapies for children. These pioneering studies using TTX as a treatment in animal models of amblyopia may help to illuminate what is needed to create a pharmacological treatment suitable for human use. Future studies will be needed in higher order mammals with compounds that act accordingly to TTX without presenting toxicity limitations.

# BIBLIOGRAPHY

Antonini, A. and M. P. Stryker (1993). "Rapid remodeling of axonal arbors in the visual cortex." Science 260(5115): 1819-1821.

Antonini, A. and M. P. Stryker (1996). "Plasticity of geniculocortical afferents following brief or prolonged monocular occlusion in the cat." J Comp Neurol 369(1): 64-82.

Antonini, A. and M. P. Stryker (1998). "Effect of sensory disuse on geniculate afferents to cat visual cortex." Vis Neurosci 15(3): 401-409.

Bane, V., M. Lehane, M. Dikshit, A. O'Riordan and A. Furey (2014). "Tetrodotoxin: chemistry, toxicity, source, distribution and detection." Toxins (Basel) 6(2): 693-755.

Bickford, M. E., W. Guido and D. W. Godwin (1998). "Neurofilament proteins in Y-cells of the cat lateral geniculate nucleus: normal expression and alteration with visual deprivation." J Neurosci 18(16): 6549-6557.

Birch, E. E. (2013). "Amblyopia and binocular vision." Prog Retin Eye Res 33: 67-84.

Bloomfield, S. A. (1996). "Effect of spike blockade on the receptive-field size of amacrine and ganglion cells in the rabbit retina." J Neurophysiol 75(5): 1878-1893.

Bode-Greuel, K. M. and W. Singer (1989). "The development of N-methyl-D-aspartate receptors in cat visual cortex." Brain Res Dev Brain Res 46(2): 197-204.

Chalupa, L. M. and R. W. Williams (1984). "Organization of the cat's lateral geniculate nucleus following interruption of prenatal binocular competition." Hum Neurobiol 3(2): 103-107.

Chapman, B., M. D. Jacobson, H. O. Reiter and M. P. Stryker (1986). "Ocular dominance shift in kitten visual cortex caused by imbalance in retinal electrical activity." Nature 324(6093): 154-156.

Chen, L., N. G. F. Cooper and G. D. Mower (2000). "Developmental changes in the expression of NMDA receptor subunits (NR1, NR2A, NR2B) in the cat visual cortex and the effects of dark rearing." Molecular Brain Research 78(1–2): 196-200.

Cooke, S. F. and M. F. Bear (2010). "Visual experience induces long-term potentiation in the primary visual cortex." J Neurosci 30(48): 16304-16313.

Cynader, M. and D. E. Mitchell (1980). "Prolonged sensitivity to monocular deprivation in dark-reared cats." J Neurophysiol 43(4): 1026-1040.

Daw, N. W., K. Fox, H. Sato and D. Czepita (1992). "Critical period for monocular deprivation in the cat visual cortex." J Neurophysiol 67(1): 197-202.

Duffy, K. R., K. D. Holman and D. E. Mitchell (2014). "Shrinkage of X cells in the lateral geniculate nucleus after monocular deprivation revealed by FoxP2 labeling." Vis Neurosci 31(3): 253-261.

Duffy, K. R., A. J. Lingley and K. D. Holman (2016). "Susceptibility to monocular deprivation following immersion in darkness either late into or beyond the critical period."

Duffy, K. R. and M. S. Livingstone (2005). "Loss of neurofilament labeling in the primary visual cortex of monocularly deprived monkeys." Cereb Cortex 15(8): 1146-1154.

Duffy, K. R. and D. E. Mitchell (2013). "Darkness alters maturation of visual cortex and promotes fast recovery from monocular deprivation." Curr Biol 23(5): 382-386.

Duffy, K. R., K. M. Murphy, M. P. Frosch and M. S. Livingstone (2007). "Cytochrome oxidase and neurofilament reactivity in monocularly deprived human primary visual cortex." Cereb Cortex 17(6): 1283-1291.

Duffy, K. R. and J. E. Slusar (2009). "Monocular deprivation provokes alteration of the neuronal cytoskeleton in developing cat lateral geniculate nucleus." Vis Neurosci 26(3): 319-328.

Dyck, R. H., A. Chaudhuri and M. S. Cynader (2003). "Experience-dependent regulation of the zincergic innervation of visual cortex in adult monkeys." Cereb Cortex 13(10): 1094-1109.

Fagiolini, M., H. Katagiri, H. Miyamoto, H. Mori, S. G. Grant, M. Mishina and T. K. Hensch (2003). "Separable features of visual cortical plasticity revealed by N-methyl-D-aspartate receptor 2A signaling." Proc Natl Acad Sci U S A 100(5): 2854-2859.

Fong, M. F., D. E. Mitchell, K. R. Duffy and M. F. Bear (2016). "Rapid recovery from the effects of early monocular deprivation is enabled by temporary inactivation of the retinas." Proc Natl Acad Sci U S A 113(49): 14139-14144.

Fonseca, R., U. V. Nagerl, R. G. Morris and T. Bonhoeffer (2004). "Competing for memory: hippocampal LTP under regimes of reduced protein synthesis." Neuron 44(6): 1011-1020.

Georges, E. and W. E. Mushynski (1987). "Chemical modification of charged amino acid moieties alters the electrophoretic mobilities of neurofilament subunits on SDS/polyacrylamide gels." Eur J Biochem 165(2): 281-287.

Greuel, J. M., H. J. Luhmann and W. Singer (1987). "Evidence for a threshold in experience-dependent long-term changes of kitten visual cortex." Brain Res 431(1): 141-149.

Guillery, R. W. (1973). "The effect of lid suture upon the growth of cells in the dorsal lateral geniculate nucleus of kittens." J Comp Neurol 148(4): 417-422.

Guillery, R. W. and D. J. Stelzner (1970). "The differential effects of unilateral lid closure upon the monocular and binocular segments of the dorsal lateral geniculate nucleus in the cat." J Comp Neurol 139(4): 413-421.

Hartig, W., A. Derouiche, K. Welt, K. Brauer, J. Grosche, M. Mader, A. Reichenbach and G. Bruckner (1999). "Cortical neurons immunoreactive for the potassium channel Kv3.1b subunit are predominantly surrounded by perineuronal nets presumed as a buffering system for cations." Brain Res 842(1): 15-29.

Headon, M. P. and T. P. Powell (1973). "Cellular changes in the lateral geniculate nucleus of infant monkeys after suture of the eyelids." J Anat 116(Pt 1): 135-145.

Hensch, T. K. (2005). "Critical period plasticity in local cortical circuits." Nat Rev Neurosci 6(11): 877-888.

Hensch, T. K., M. Fagiolini, N. Mataga, M. P. Stryker, S. Baekkeskov and S. F. Kash (1998). "Local GABA circuit control of experience-dependent plasticity in developing visual cortex." Science 282(5393): 1504-1508.

Hensch, T. K. and M. P. Stryker (2004). "Columnar architecture sculpted by GABA circuits in developing cat visual cortex." Science 303(5664): 1678-1681.

Hoffmann, K. P., J. Stone and S. M. Sherman (1972). "Relay of receptive-field properties in dorsal lateral geniculate nucleus of the cat." J Neurophysiol 35(4): 518-531.

Huang, Z. J., A. Kirkwood, T. Pizzorusso, V. Porciatti, B. Morales, M. F. Bear, L. Maffei and S. Tonegawa (1999). "BDNF regulates the maturation of inhibition and the critical period of plasticity in mouse visual cortex." Cell 98(6): 739-755.

Hubel, D. H. and T. N. Wiesel (1959). "Receptive fields of single neurones in the cat's striate cortex." J Physiol 148(3): 574-591.

Hubel, D. H. and T. N. Wiesel (1962). "Receptive fields, binocular interaction and functional architecture in the cat's visual cortex." J Physiol 160(1): 106-154.102.

Hubel, D. H. and T. N. Wiesel (1963). "Receptive fields of cells in striate cortex of very young, visually inexperienced kittens." J Neurophysiol 26: 994-1002.

Hubel, D. H. and T. N. Wiesel (1965). "Binocular interaction in striate cortex of kittens reared with artificial squint." J Neurophysiol 28(6): 1041-1059.

Hubel, D. H. and T. N. Wiesel (1970). "The period of susceptibility to the physiological effects of unilateral eye closure in kittens." J Physiol 206(2): 419-436.

Julien, J. P. and W. E. Mushynski (1982). "Multiple phosphorylation sites in mammalian neurofilament polypeptides." J Biol Chem 257(17): 10467-10470.

Kaufmann, E., N. Geisler and K. Weber (1984). "SDS-PAGE strongly overestimates the molecular masses of the neurofilament proteins." FEBS Lett 170(1): 81-84.

Kerr, J. F., A. H. Wyllie and A. R. Currie (1972). "Apoptosis: a basic biological phenomenon with wide-ranging implications in tissue kinetics." Br J Cancer 26(4): 239-257.

Kutcher, M. R. and K. R. Duffy (2007). "Cytoskeleton alteration correlates with gross structural plasticity in the cat lateral geniculate nucleus." Vis Neurosci 24(6): 775-785.

Lavenex, P., P. B. Lavenex and D. G. Amaral (2004). "Nonphosphorylated high-molecular-weight neurofilament expression suggests early maturation of the monkey subiculum." Hippocampus 14(7): 797-801.

Lee, S. and T. B. Shea (2014). "The high molecular weight neurofilament subunit plays an essential role in axonal outgrowth and stabilization." Biol Open 3(10): 974-981.

LeVay, S. and D. Ferster (1977). "Relay cell classes in the lateral geniculate nucleus of the cat and the effects of visual deprivation." J Comp Neurol 172(4): 563-584.

LeVay, S., M. P. Stryker and C. J. Shatz (1978). "Ocular dominance columns and their development in layer IV of the cat's visual cortex: a quantitative study." J Comp Neurol 179(1): 223-244.

Mansouri, B., R. C. Stacy, J. Kruger and D. M. Cestari (2013). "Deprivation amblyopia and congenital hereditary cataract." Semin Ophthalmol 28(5-6): 321-326.

Mataga, N., Y. Mizuguchi and T. K. Hensch (2004). "Experience-dependent pruning of dendritic spines in visual cortex by tissue plasminogen activator." Neuron 44(6): 1031-1041.

Mitchell, D. E. (1988). "The extent of visual recovery from early monocular or binocular visual deprivation in kittens." J Physiol 395: 639-660.

Mitchell, D. E. (1989). "Normal and abnormal visual development in kittens: insights into the mechanisms that underlie visual perceptual development in humans." Can J Psychol 43(2): 141-164.

Mitchell, D. E., M. Cynader and J. A. Movshon (1977). "Recovery from the effects of monocular deprivation in kittens." J Comp Neurol 176(1): 53-63.

Mitchell, D. E. and K. R. Duffy (2014). "The case from animal studies for balanced binocular treatment strategies for human amblyopia." Ophthalmic Physiol Opt 34(2): 129-145.

Mitchell, D. E., J. Kennie and K. R. Duffy (2011). "Preference for binocular concordant visual input in early postnatal development remains despite prior monocular deprivation." Vision Res 51(12): 1351-1359.

Mower, G. D., D. Berry, J. L. Burchfiel and F. H. Duffy (1981). "Comparison of the effects of dark rearing and binocular suture on development and plasticity of cat visual cortex." Brain Res 220(2): 255-267.

Mower, G. D., J. L. Burchfiel and F. H. Duffy (1981). "The effects of dark-rearing on the development and plasticity of the lateral geniculate nucleus." Brain Res 227(3): 418-424.

Mower, G. D. and W. G. Christen (1985). "Role of visual experience in activating critical period in cat visual cortex." J Neurophysiol 53(2): 572-589.

Myers, M. W., R. A. Lazzarini, V. M. Lee, W. W. Schlaepfer and D. L. Nelson (1987). "The human mid-size neurofilament subunit: a repeated protein sequence and the relationship of its gene to the intermediate filament gene family." Embo j 6(6): 1617-1626.

Nys, J., I. Scheyltjens and L. Arckens (2015). "Visual system plasticity in mammals: the story of monocular enucleation-induced vision loss." Front Syst Neurosci 9: 60.

O'Leary, T. P., M. R. Kutcher, D. E. Mitchell and K. R. Duffy (2012). "Recovery of neurofilament following early monocular deprivation." Front Syst Neurosci 6: 22.

Olson, C. R. and R. D. Freeman (1980). "Profile of the sensitive period for monocular deprivation in kittens." Exp Brain Res 39(1): 17-21.

Philpot, B. D., K. K. Cho and M. F. Bear (2007). "Obligatory role of NR2A for metaplasticity in visual cortex." Neuron 53(4): 495-502.

Pizzorusso, T., P. Medini, N. Berardi, S. Chierzi, J. W. Fawcett and L. Maffei (2002). "Reactivation of ocular dominance plasticity in the adult visual cortex." Science 298(5596): 1248-1251.

Quinlan, E. M., D. H. Olstein and M. F. Bear (1999). "Bidirectional, experience-dependent regulation of N-methyl-D-aspartate receptor subunit composition in the rat visual cortex during postnatal development." Proc Natl Acad Sci U S A 96(22): 12876-12880.

Quinlan, E. M., B. D. Philpot, R. L. Huganir and M. F. Bear (1999). "Rapid, experience-dependent expression of synaptic NMDA receptors in visual cortex in vivo." Nat Neurosci 2(4): 352-357.

Rauschecker, J. P. (1991). "Mechanisms of visual plasticity: Hebb synapses, NMDA receptors, and beyond." Physiol Rev 71(2): 587-615.

Reiter, H. O., D. M. Waitzman and M. P. Stryker (1986). "Cortical activity blockade prevents ocular dominance plasticity in the kitten visual cortex." Exp Brain Res 65(1): 182-188.

Sanderson, K. J. (1971). "The projection of the visual field to the lateral geniculate and medial interlaminar nuclei in the cat." J Comp Neurol 143(1): 101-108.

Shatz, C. J. and M. P. Stryker (1978). "Ocular dominance in layer IV of the cat's visual cortex and the effects of monocular deprivation." J Physiol 281: 267-283.

Song, S., D. E. Mitchell, N. A. Crowder and K. R. Duffy (2015). "Postnatal accumulation of intermediate filaments in the cat and human primary visual cortex." J Comp Neurol 523(14): 2111-2126.

Stryker, M. P. and W. A. Harris (1986). "Binocular impulse blockade prevents the formation of ocular dominance columns in cat visual cortex." J Neurosci 6(8): 2117-2133.

Teyler, T. J. and S. B. Fountain (1987). "Neuronal plasticity in the mammalian brain: relevance to behavioral learning and memory." Child Dev 58(3): 698-712.

Trachtenberg, J. T., C. Trepel and M. P. Stryker (2000). "Rapid extragranular plasticity in the absence of thalamocortical plasticity in the developing primary visual cortex." Science 287(5460): 2029-2032.

Tsumoto, T., K. Hagihara, H. Sato and Y. Hata (1987). "NMDA receptors in the visual cortex of young kittens are more effective than those of adult cats." Nature 327(6122): 513-514.

Wallace, M. P., C. E. Stewart, M. J. Moseley, D. A. Stephens and A. R. Fielder (2013). "Compliance with occlusion therapy for childhood amblyopia." Invest Ophthalmol Vis Sci 54(9): 6158-6166.

Whitlock, J. R., A. J. Heynen, M. G. Shuler and M. F. Bear (2006). "Learning induces long-term potentiation in the hippocampus." Science 313(5790): 1093-1097.

Wiesel, T. N. and D. H. Hubel (1963). "Effects of visual deprivation on morphology and physiology of cells in the cats lateral geniculate body." J Neurophysiol 26: 978-993.

Wiesel, T. N. and D. H. Hubel (1963). "Single-cell responses in striate cortex of kittens deprived of vision in one eye." J Neurophysiol 26: 1003-1017.

Wiesel, T. N. and D. H. Hubel (1965). "Extent of recovery from the effects of visual deprivation in kittens." J Neurophysiol 28(6): 1060-1072.

Wong, A. M. (2012). "New concepts concerning the neural mechanisms of amblyopia and their clinical implications." Can J Ophthalmol 47(5): 399-409.

# APPENDIX A - TABLES

Table 1. Absolute values ($\mu m^2$), averages ($\mu m^2$), and deprivation indexes from stereological measurements of neuron somata size within layers A and A1 of both the left and right dLGN.

| Animal | Condition | Left A1 | Left A | Right A1 | Right A | Dep Ave | Non-Dep Ave | Dep Index |
|---|---|---|---|---|---|---|---|---|
| C345 | 7d MD + 10d Binoc TTX | 131.565 | 110.376 | 134.051 | 117.860 | 124.713 | 122.213 | -0.021 |
| C382 | 7d MD + 10d Binoc TTX | 180.885 | 149.937 | 153.559 | 136.625 | 158.755 | 151.748 | -0.046 |
| C398 | 7d MD + 10d Binoc TTX | 199.648 | 170.136 | 173.666 | 163.267 | 181.457 | 171.901 | -0.056 |
| C342 | 7d MD + 10d Monoc TTX | 98.520 | 152.154 | 163.576 | 93.617 | 96.069 | 157.865 | 0.391 |
| C348 | 7d MD + 10d Monoc TTX | 140.312 | 185.972 | 243.243 | 146.839 | 143.574 | 214.608 | 0.331 |
| C400 | 7d MD + 10d Monoc TTX | 154.239 | 235.076 | 252.368 | 156.04 | 155.139 | 243.722 | 0.363 |
| C380 | 7d MD + 6d Binoc TTX | 184.988 | 193.621 | 207.514 | 176.453 | 180.720 | 200.567 | 0.099 |
| C367 | 7d MD + 4d Binoc TTX | 157.242 | 187.461 | 216.497 | 183.988 | 170.615 | 201.979 | 0.155 |
| C370 | 7d MD + 4d Binoc TTX | 128.35 | 148.194 | 142.438 | 136.554 | 132.452 | 145.318 | 0.089 |
| C384 | P47 Normal | 179.463 | 164.117 | 189.40 | 158.953 | 169.208 | 176.758 | 0.043 |
| C385 | P47 Normal | 181.811 | 154.821 | 151.743 | 133.428 | 157.62 | 153.282 | -0.028 |
| C386 | P47 Normal | 259.569 | 212.95 | 227.296 | 172.698 | 215.862 | 220.123 | 0.019 |
| C244 | P47 Normal | 279.569 | 223.851 | 258.557 | 247.208 | 263.389 | 241.204 | -0.092 |
| C242 | 7d MD | 178.157 | 199.376 | 219.747 | 172.54 | 175.348 | 209.561 | 0.163 |
| C243 | 7d MD | 178.919 | 195.12 | 210.172 | 155.451 | 167.185 | 202.646 | 0.175 |

Table 2. Absolute values (neurons/mm$^2$), averages (neurons/mm$^2$), and deprivation indexes from stereological measurements of NF-H density within layers A and A1 of both the left and right dLGN.

| Animal | Condition | Left A1 | Left A | Right A1 | Right A | Dep Ave | Non-Dep Ave | Dep Index |
|---|---|---|---|---|---|---|---|---|
| C345 | 7d MD + 10d Binoc TTX | 249.981 | 226.172 | 280.354 | 221.687 | 235.834 | 253.263 | 0.069 |
| C398 | 7d MD + 10d Binoc TTX | 221.668 | 174.349 | 231.770 | 204.753 | 213.210 | 203.060 | -0.050 |
| C342 | 7d MD + 10d Monoc TTX | 181.902 | 227.116 | 277.515 | 159.896 | 170.899 | 252.315 | 0.323 |
| C400 | 7d MD + 10d Monoc TTX | 278.002 | 445.806 | 314.641 | 275.516 | 276.759 | 380.223 | 0.272 |
| C380 | 7d MD + 6d Binoc TTX | 294.855 | 206.919 | 259.376 | 202.750 | 248.802 | 233.147 | -0.067 |
| C367 | 7d MD + 4d Binoc TTX | 174.556 | 237.105 | 188.412 | 174.219 | 174.387 | 212.759 | 0.180 |
| C370 | 7d MD + 4d Binoc TTX | 161.435 | 244.153 | 179.649 | 186.783 | 174.109 | 211.901 | 0.178 |
| C384 | P47 Normal | 235.033 | 253.622 | 227.993 | 226.018 | 230.525 | 240.807 | 0.043 |
| C385 | P47 Normal | 166.464 | 104.154 | 154.259 | 87.427 | 126.946 | 129.207 | 0.018 |
| C386 | P47 Normal | 144.538 | 123.756 | 181.369 | 163.600 | 154.069 | 152.563 | -0.010 |
| C242 | 7d MD | 270.583 | 365.741 | 300.405 | 283.714 | 277.149 | 333.073 | 0.168 |
| C243 | 7d MD | 240.446 | 244.244 | 317.126 | 170.637 | 205.541 | 280.685 | 0.268 |

## APPENDIX B – FIGURES

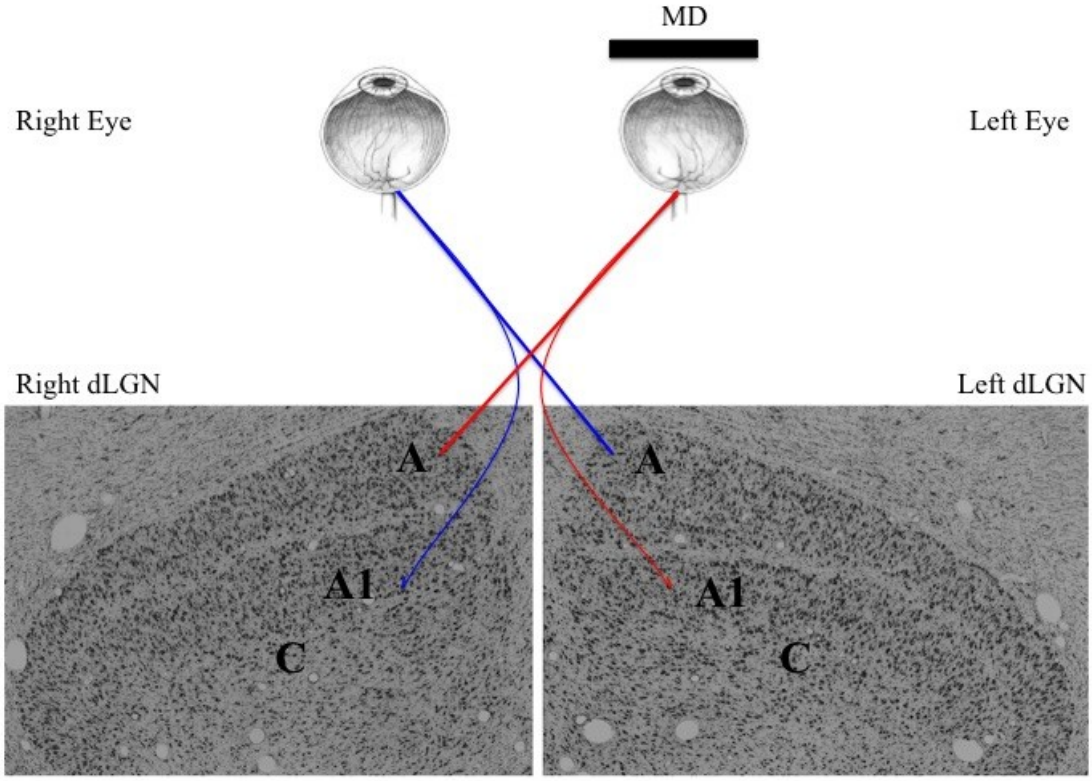

Figure 1. Simplified diagram of the retinogeniculate visual pathway.
Projections from the retina of each eye follow the optic tract to the dorsal lateral geniculate nucleus (dLGN). The dLGN comprises 3 layers; A, A1 and C. Layers A and A1 are monocular; therefore they receive input from either the right or left eye. This diagram shows the results of monocular deprivation of the left eye. The red layers (right A and left A1) will be deprived as they receive input from the left, deprived eye. The blue layers (left A and right A1) will not be deprived as they receiver input from the right, non-deprived eye. All subsequent photomicrographs will take this format, as it is consistent with general practice.

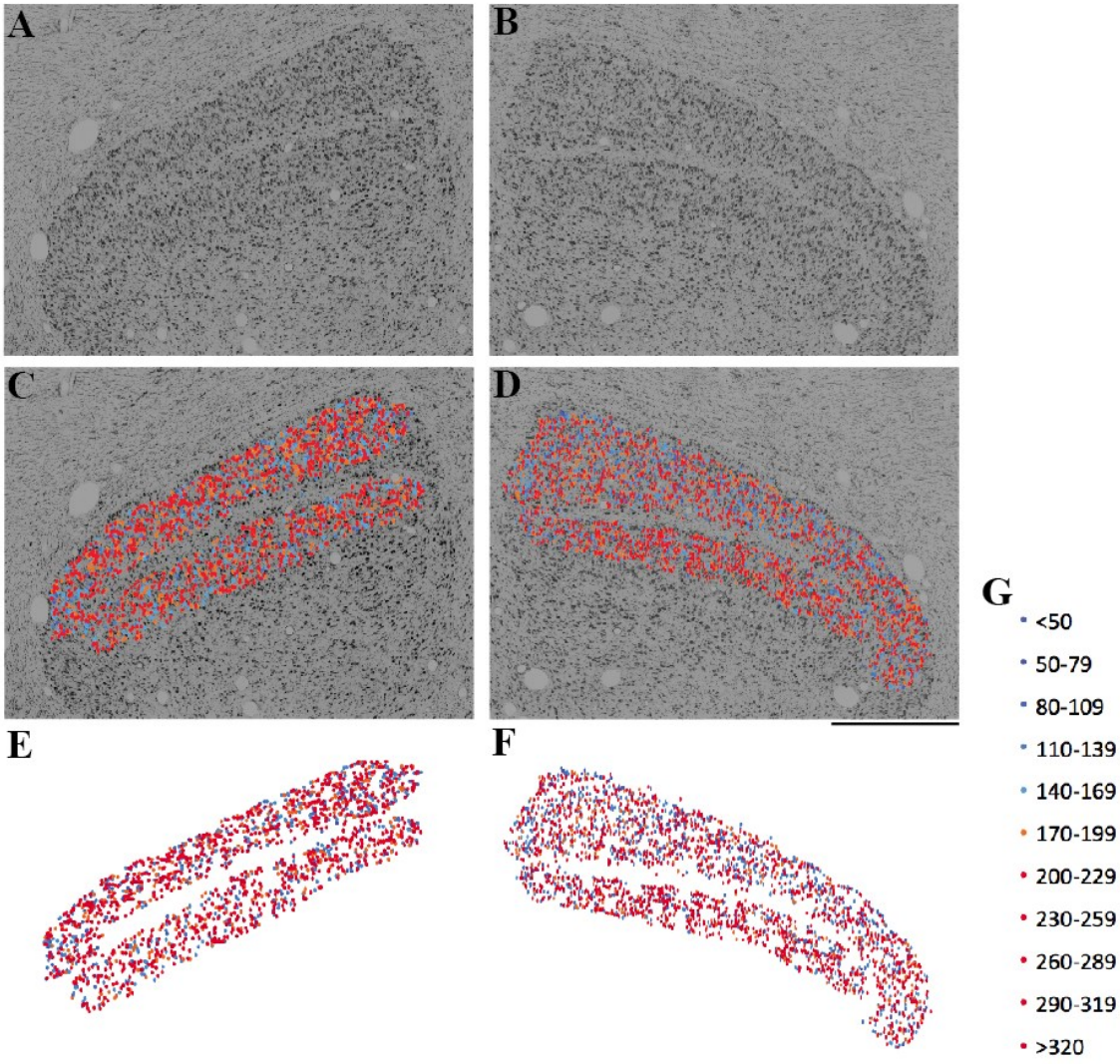
A
B
C
D
E
F
G
<50
50-79
80-109
110-139
140-169
170-199
200-229
230-259
260-289
290-319
>320

Figure 2. Animals reared normally to P47 exhibit normal anatomical development, consistent with previous studies, in the dLGN. This is kitten C384. **A & B**: Neurons within left-eye layers (LA1 & RA) were indistinguishable from those in right-eye layers (LA & RA1) in appearance, apparent size and distribution. **C & D**: 2-D colour-coded scatterplots of the left and right dLGN were aligned to the photomicrograph to reveal position and size of neuron somata within layers for normally reared kittens. Both the left and right Nissl stained dLGNs exhibit a normal balance of neuronal soma size. Animals reared normally to P47 did not exhibit any retinotopic changes in that there was a balance of cell size between the medial binocular segment and the lateral monocular segment. **E & F:** 2-D colour-coded scatterplots of the left and right dLGN. **G:** Bins of neuron somata size ($\mu m^2$) and corresponding colour. Scale bar = 1 mm.

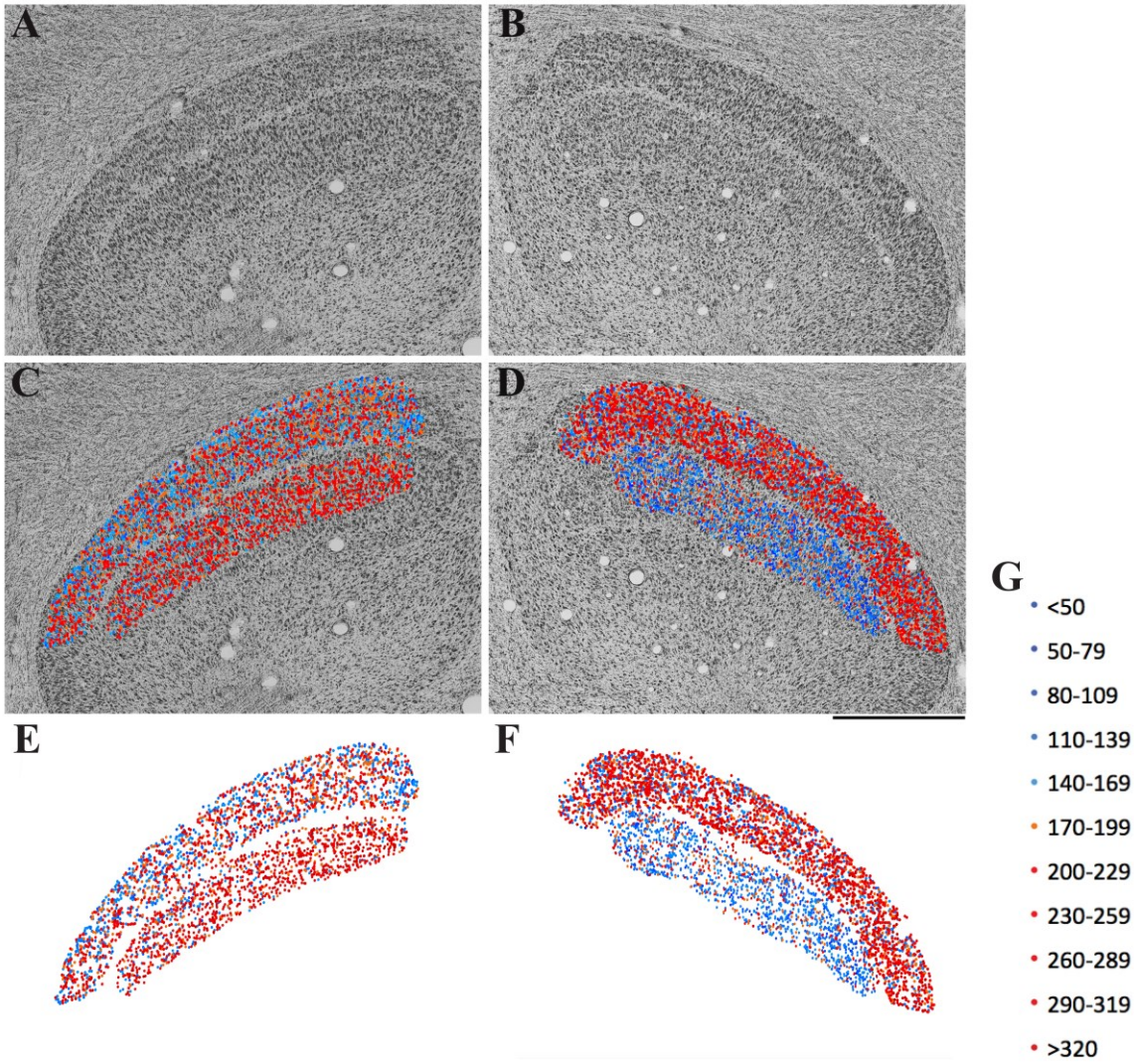
A
B
C
D
E
F
G
<50
50-79
80-109
110-139
140-169
170-199
200-229
230-259
260-289
290-319
>320

Figure 3. Neuronal alterations within the left and right dLGN of a kitten (C242) following a period of MD from P30-P37 in the left eye. **A & B**: Neurons within deprived layers (LA1 & RA) were altered compared to from those in non-deprived layers (LA & RA1) in appearance, apparent size and distribution. **C & D**: 2-D colour-coded scatterplots of the left and right dLGN were aligned to the photomicrograph to reveal position and size of neuron somata within layers. Both the left and right Nissl stained dLGNs exhibit atrophy of neurons within the deprived layers. Neurons located in the medial binocular segment were more affected by MD than those found in the lateral monocular segment.
**E & F:** 2-D colour-coded scatterplots of the left and right dLGN. **G:** Bins of neuron somata size ($\mu m^2$) and corresponding colour. Scale bar = 1 mm.

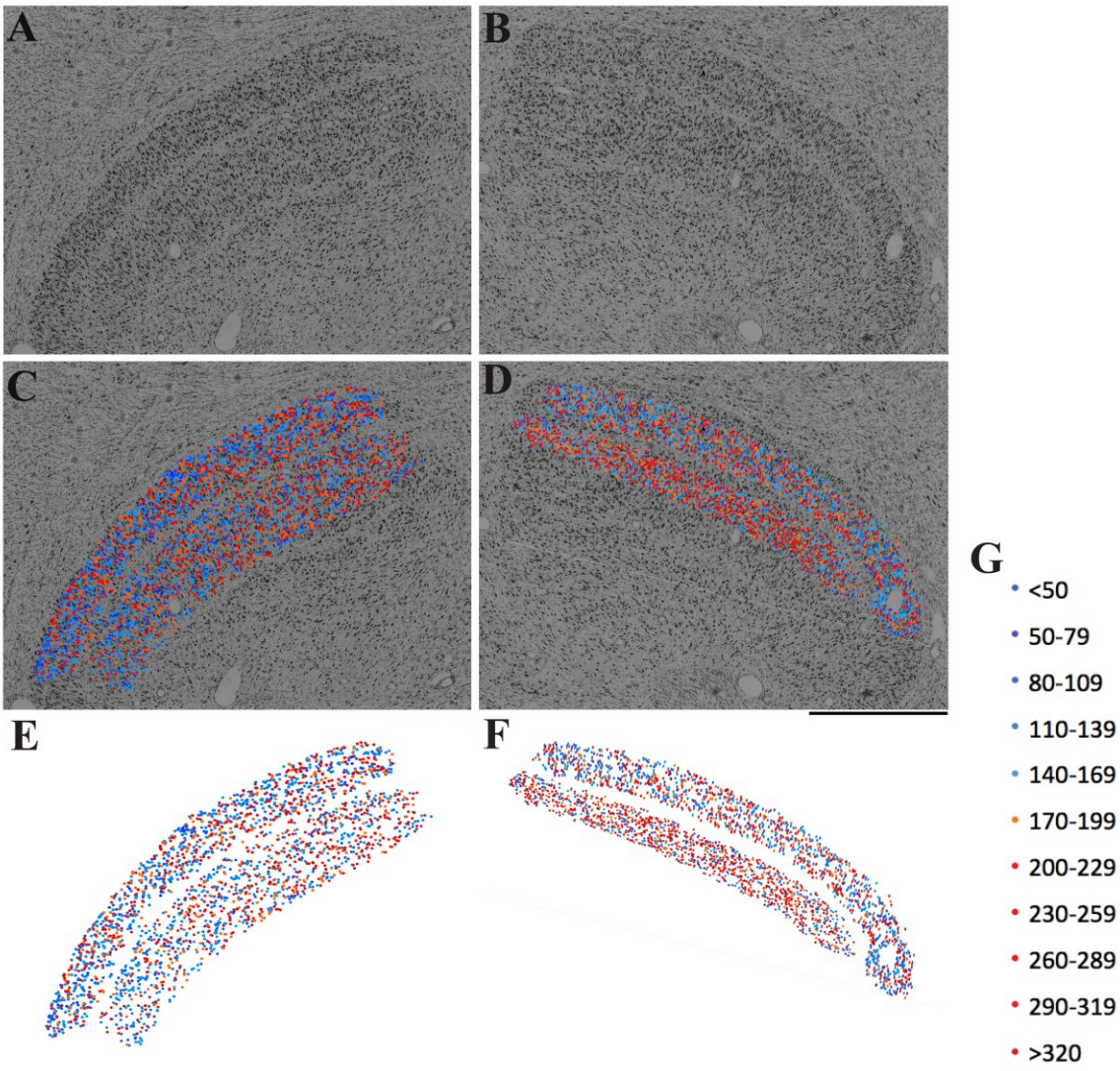
A
B
C
D
E
F
G
<50
50-79
80-109
110-139
140-169
170-199
200-229
230-259
260-289
290-319
>320

Figure 4. Neuronal alterations within the left and right dLGN of a kitten (C398) precipitated by a 10-day period of binocular retinal inactivation following MD from P30-P37. **A & B**: Neurons within deprived layers (LA1 & RA) were indistinguishable to those in non-deprived layers (LA & RA1) in appearance, apparent size and distribution. **C & D**: 2-D colour-coded scatterplots of the left and right dLGN were aligned to the photomicrograph to reveal position and size of neuron somata within layers. Both the left and right Nissl stained dLGNs exhibit a balance of neuron somata size between the deprived and non-deprived layers similar to that of normal animals. Neuron soma sizes in the medial binocular segment were equivalent to those measured in the lateral monocular segment. **E & F:** 2-D colour-coded scatterplots of the left and right dLGN. **G:** Bins of neuron somata size ($\mu m^2$) and corresponding colour. Scale bar = 1 mm.

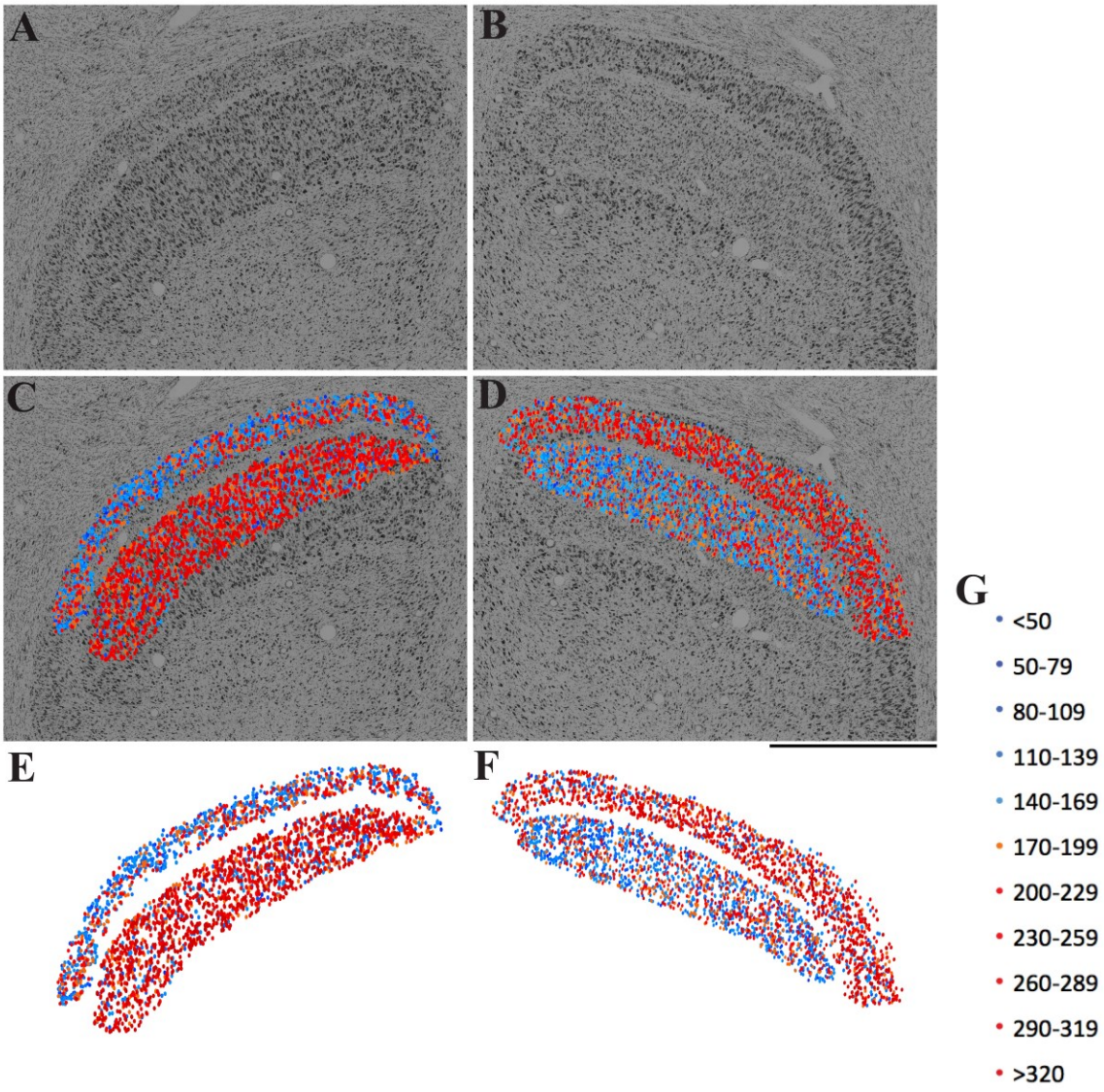
A
B
C
D
E
F
G
<50
50-79
80-109
110-139
140-169
170-199
200-229
230-259
260-289
290-319
>320

Figure 5. Neuronal alterations within the left and right dLGN of a kitten (C400) precipitated by a 10-day period of monocular retinal inactivation following MD from P30-P37. **A & B**: Neurons within deprived layers (LA1 & RA) were altered compared to those in non-deprived layers (LA & RA1) in appearance, apparent size and distribution. **C & D**: 2-D colour-coded scatterplots of the left and right dLGN were aligned to the photomicrograph to reveal position and size of neuron somata within layers. Both the left and right Nissl stained dLGNs exhibit atrophy of neurons within the deprived layers. Neurons located in the medial binocular segment were more affected than those found in the lateral monocular segment. **E & F:** 2-D colour-coded scatterplots of the left and right dLGN. **G:** Bins of neuron somata size ($\mu m^2$) and corresponding colour. Scale bar = 1 mm.

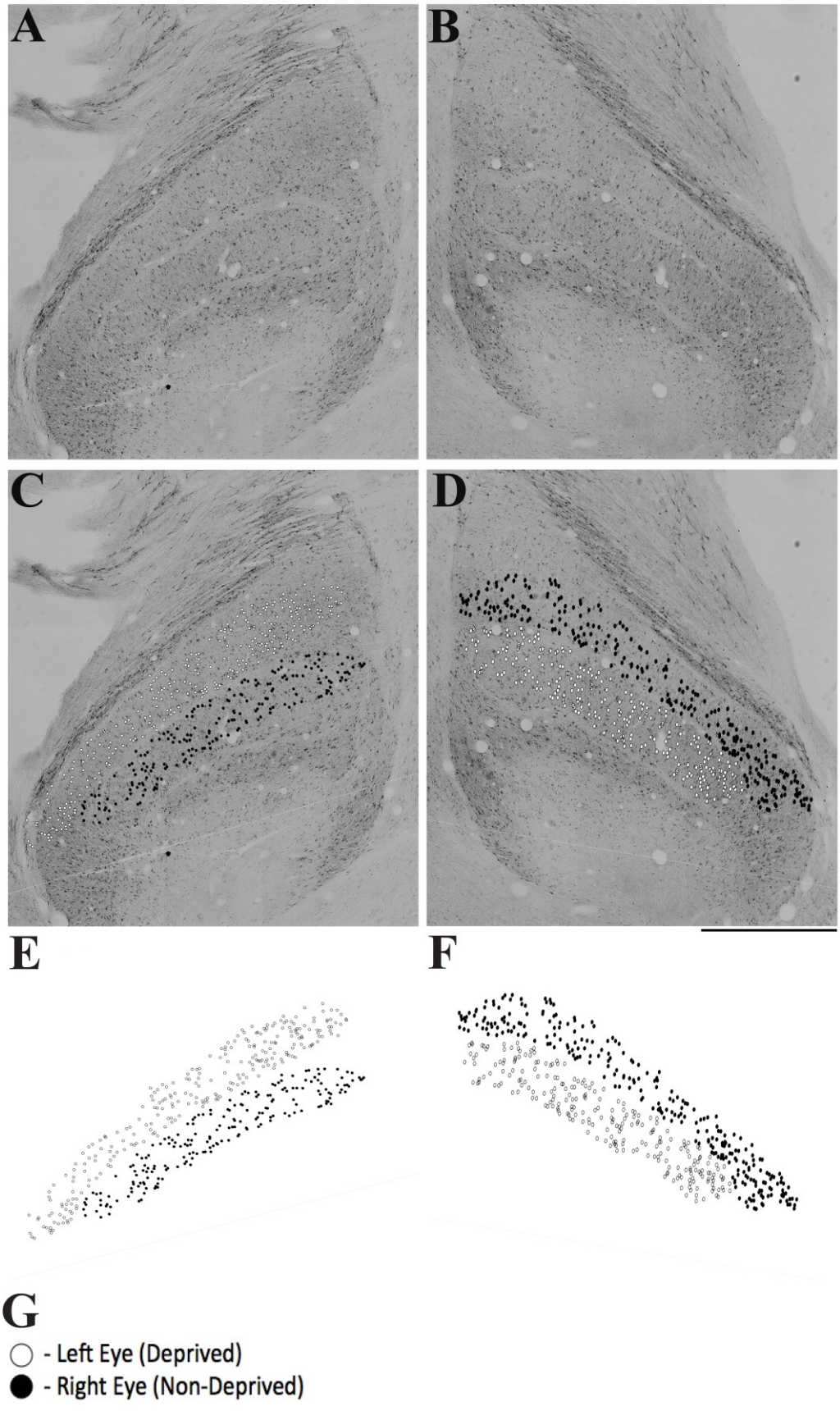
A
B
C
D
E
F
G
- Left Eye (Deprived)
- Right Eye (Non-Deprived)

Figure 6. Animals reared normally to P47 exhibit normal NF-H immunoreactivity consistent with previous studies within the dLGN. This is kitten C384. **A & B**: Neurofilament immunoreactivity was indistinguishable between left-eye (right A and left A1) and right-eye layers (left A and right A1). **C & D**: A scatterplot was aligned to the photomicrograph to reveal NF-H density. Both the left and right dLGNs exhibit a balance of NF-H labeling between layers. **E & F:** Scatterplots of NF-H density in the left and right dLGN. **G:** Legend indicating layer input from the left or right eye. Scale bar = 1 mm.

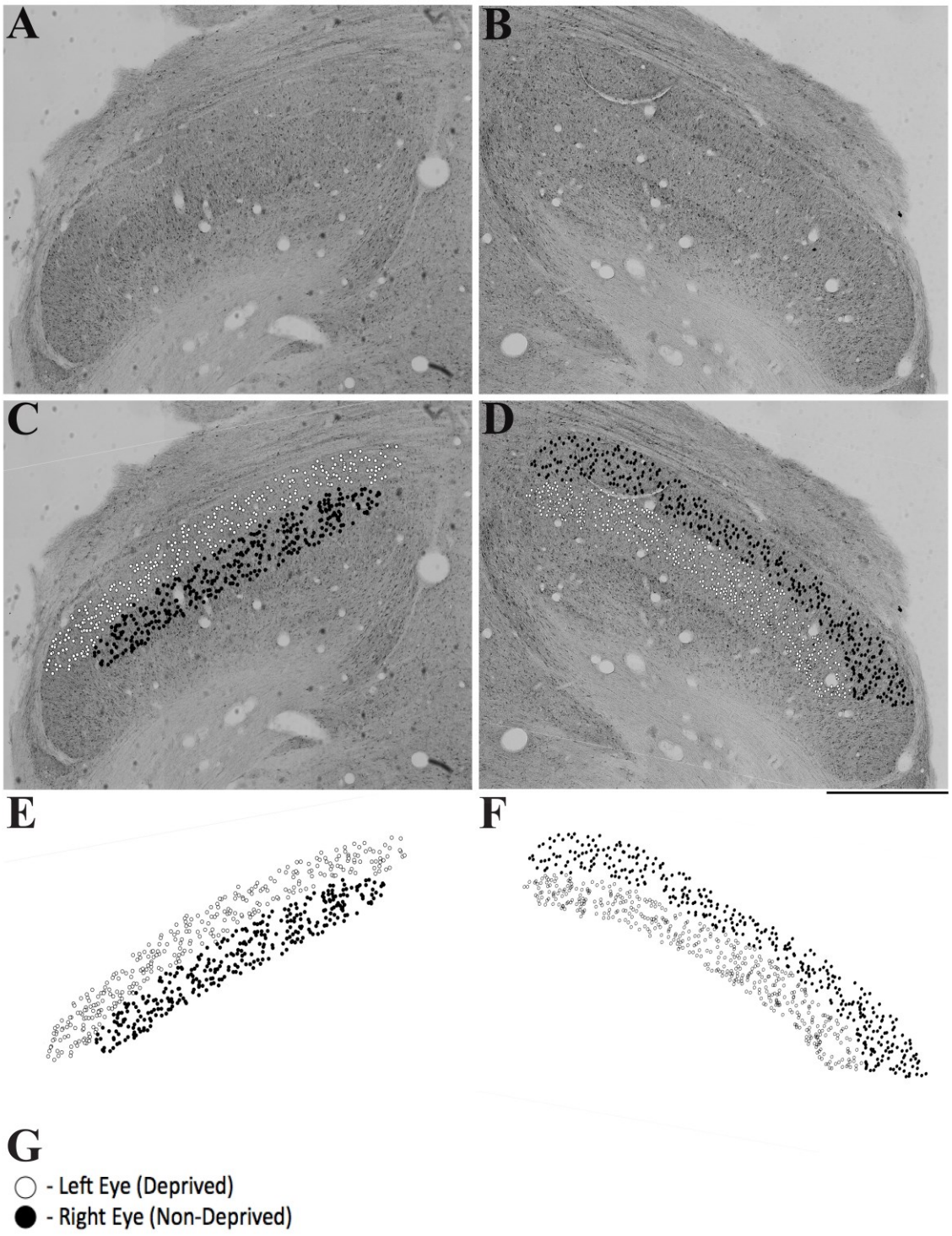
A
B
C
D
E
F
G
- Left Eye (Deprived)
- Right Eye (Non-Deprived)

Figure 7. Neurofilament-H density in the dLGN of a kitten (C242) that underwent a period of MD from P30-P37. **A & B**: Neurofilament immunoreactivity was decreased in the deprived, left-eye layers (right A and left A1) compared to the non-deprived, right-eye layers (left A and right A1). **C & D**: A scatterplot was aligned to the photomicrograph to reveal NF-H density. Both the left and right dLGNs exhibit a decrease of NF-H labeling in the deprived layers. **E & F:** Scatterplots of NF-H density in the left and right dLGN. **G:** Legend indicating layer input from the left or right eye. Scale bar = 1 mm.

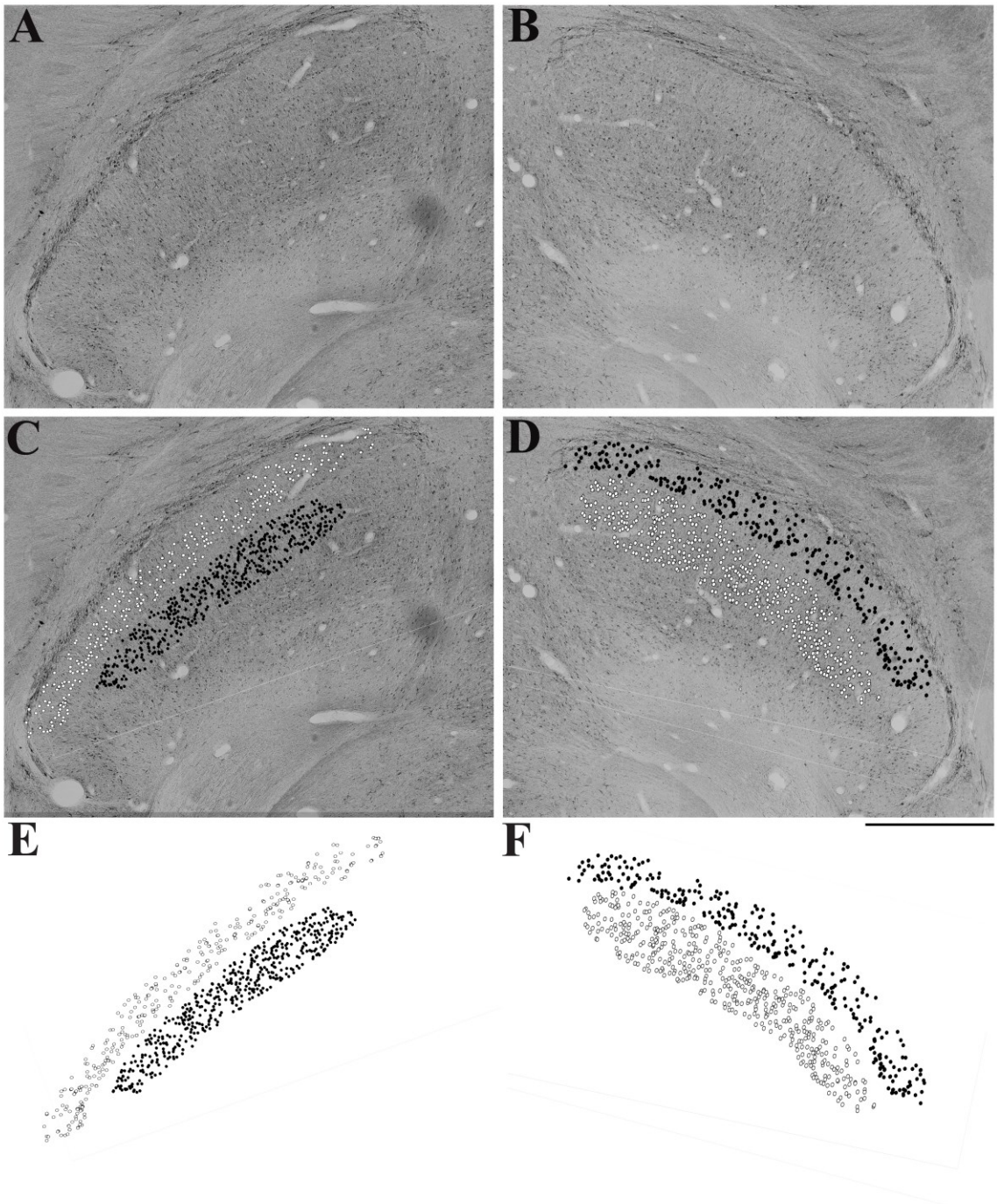
A
B
C
D
E
F
G
- Left Eye (Deprived)
- Right Eye (Non-Deprived)

Figure 8. Neurofilament-H density in the dLGN of a kitten (C398) that underwent a 10-day period of binocular retinal inactivation following a period of MD from P30-P37. **A & B**: Neurofilament immunoreactivity was balanced between the deprived, left-eye layers (right A and left A1) and the non-deprived, right-eye layers (left A and right A1). **C & D**: A scatterplot was aligned to the photomicrograph to reveal NF-H density. Both the left and right dLGNs exhibit a balance of NF-H labeling between layers. **E & F:** Scatterplots of NF-H density in the left and right dLGN. **G:** Legend indicating layer input from the left or right eye. Scale bar = 1 mm.

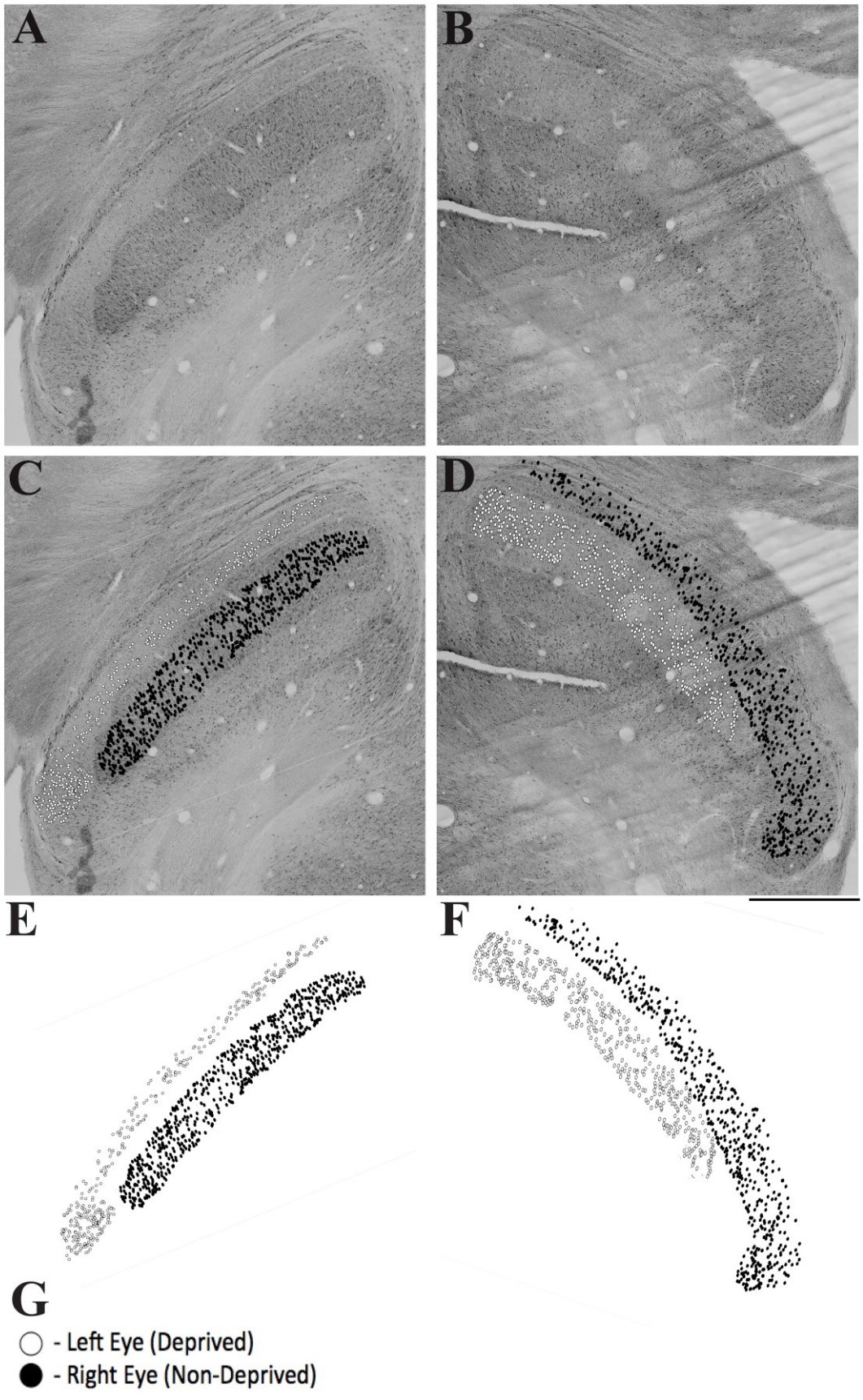
A
B
C
D
E
F
G
○ - Left Eye (Deprived)
● - Right Eye (Non-Deprived)

Figure 9. Neurofilament-H density in the dLGN of a kitten (C400) that underwent a 10-day period of monocular retinal inactivation following a period of MD from P30-P37. **A & B**: Neurofilament immunoreactivity was decreased in the deprived, left-eye layers (right A and left A1) compared to the non-deprived, right-eye layers (left A and right A1). **C & D**: A scatterplot was aligned to the photomicrograph to reveal NF-H density. Both the left and right dLGNs exhibit a decrease of NF-H labeling in the deprived layers. **E & F:** Scatterplots of NF-H density in the left and right dLGN. **G:** Legend indicating layer input from the left or right eye. Scale bar = 1 mm.

A

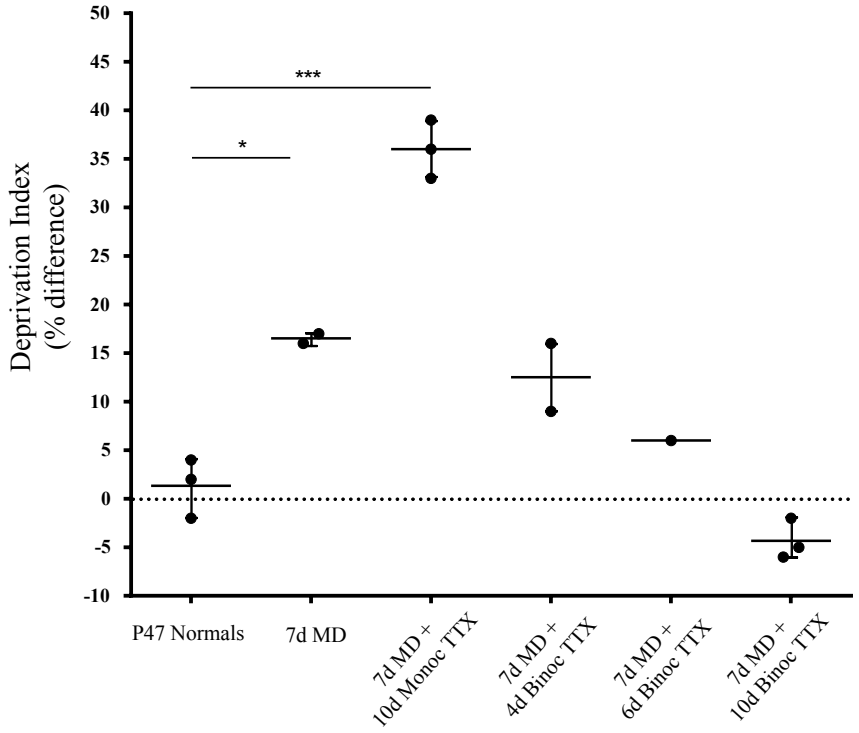
Deprivation Index
(% difference)
50
45
40
35
30
25
20
15
10
5
0
-5
-10
***
*
P47 Normals
7d MD
7d MD + 10d Monoc TTX
7d MD + 4d Binoc TTX
7d MD + 6d Binoc TTX
7d MD + 10d Binoc TTX

B

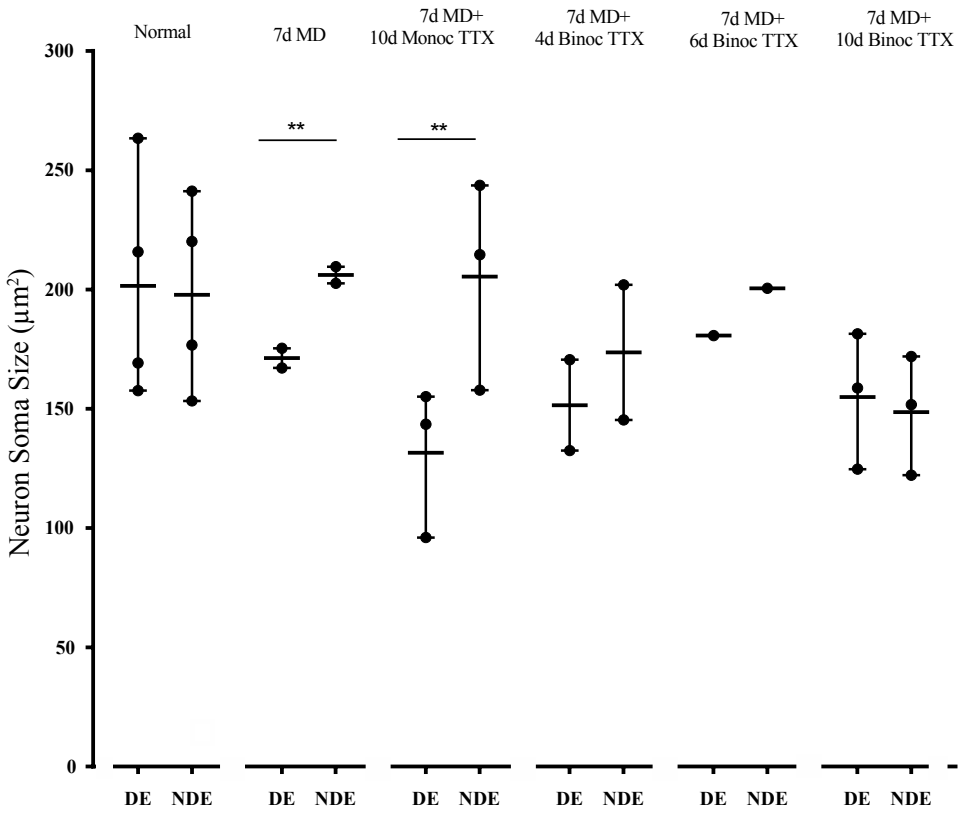
Normal
7d MD
7d MD+ 10d Monoc TTX
7d MD+ 4d Binoc TTX
7d MD+ 6d Binoc TTX
7d MD+ 10d Binoc TTX
Neuron Soma Size (μm²)
300
250
200
150
100
50
0
**
**
DE
NDE

Figure 10. Anatomical recovery seen in the kitten dLGN via Nissl staining for each animal and condition. **A**: Stereological quantification of neuron soma size within the deprived and non-deprived layers of the left and right dLGN (deprivation index, DI) revealed that following MD, only 10-days of binocular retinal inactivation with TTX was capable of inducing anatomical recovery. Dashed line represents deprivation index of normal kittens. **B**: Average left (DE) and right (NDE) eye neuron soma size for each animal and condition. Restoration of balanced neuron soma size induced by binocular retinal inactivation was the product of recovery (*** $p < 0.0005$, ** $p < 0.005$, * $p < 0.05$).

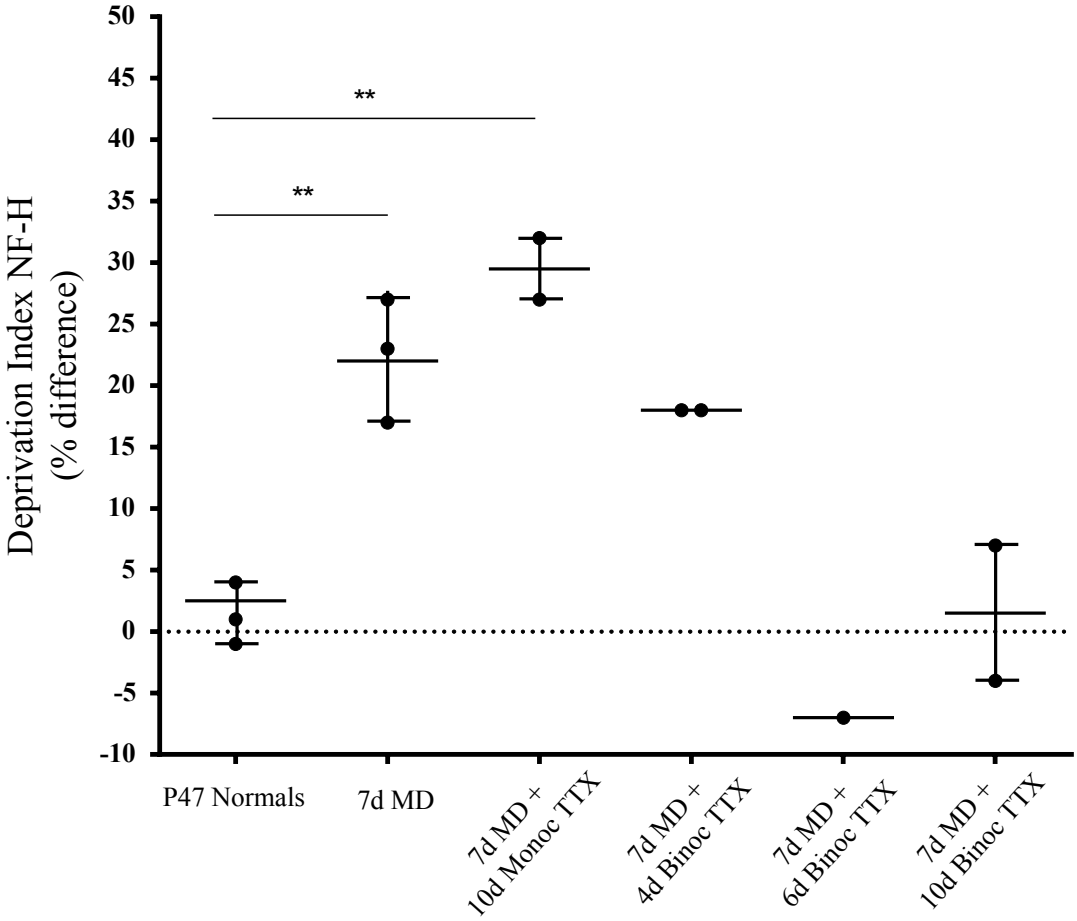
Deprivation Index NF-H
(% difference)
50
45
40
35
30
25
20
15
10
5
0
-5
-10
**
**
P47 Normals
7d MD
7d MD + 10d Monoc TTX
7d MD + 4d Binoc TTX
7d MD + 6d Binoc TTX
7d MD + 10d Binoc TTX

Figure 11. Neurofilament immunoreactivity in the dLGN of kittens within each condition. Ten days of binocular retinal inactivation in kittens immediately following MD promotes a balance in neurofilament labeling in the dLGN similar to that of normal animals. Stereological quantification of neurofilament-positive neuron density within the deprived and non-deprived layers of the left and right dLGN (deprivation index, DI) revealed that following a 7-day period of MD, 10 days of binocular retinal inactivation by way of TTX induces a balance of neurofilament-positive neurons by day 10. Dashed line represents deprivation index of normal kittens (*** $p < 0.0005$, ** $p < 0.005$, * $p < 0.05$).

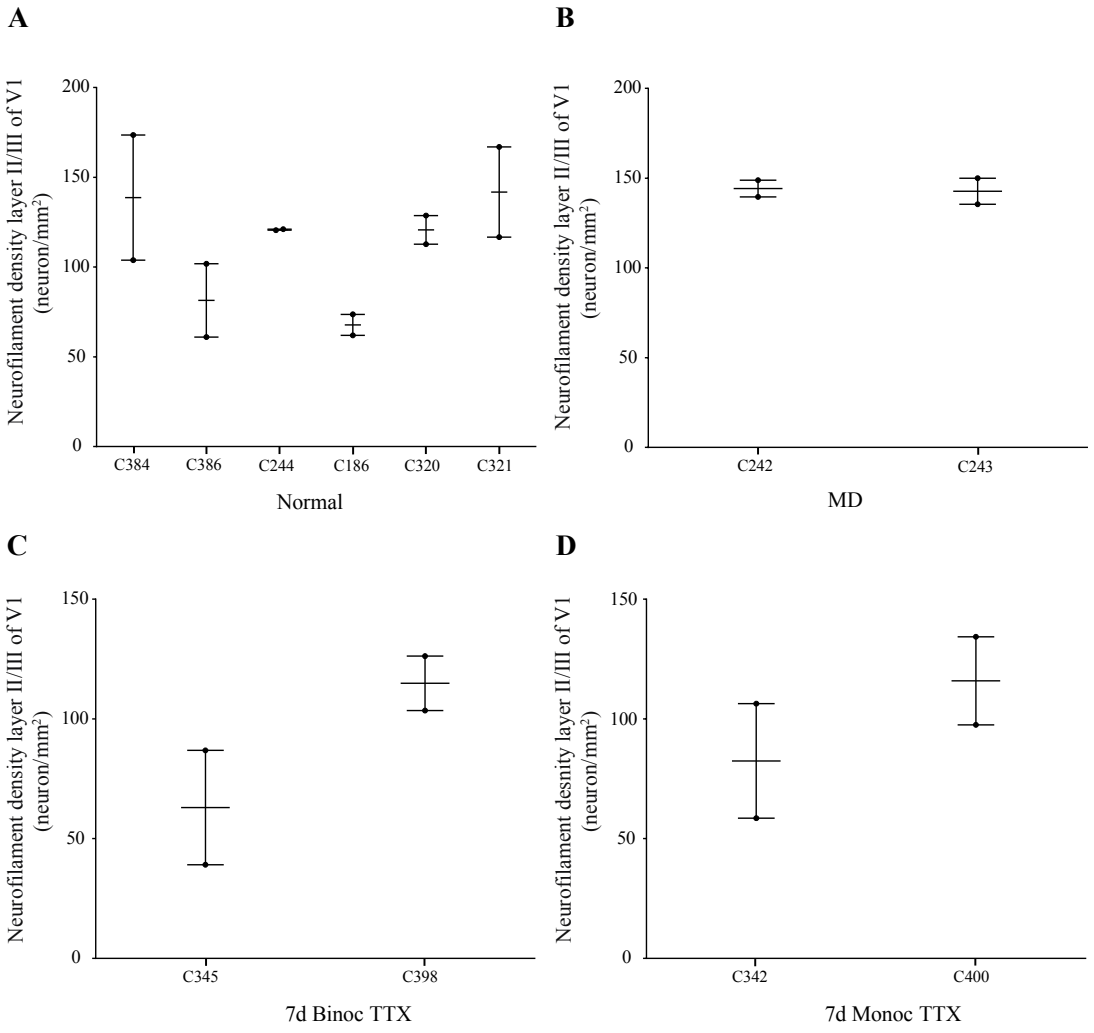
A
Neurofilament density layer II/III of V1 (neuron/mm²)
200
150
100
50
0
C384
C386
C244
C186
C320
C321
Normal
B
Neurofilament density layer II/III of V1 (neuron/mm²)
200
150
100
50
0
C242
C243
MD
C
Neurofilament density layer II/III of V1 (neuron/mm²)
150
100
50
0
C345
C398
7d Binoc TTX
D
Neurofilament desnity layer II/III of V1 (neuron/mm²)
150
100
50
0
C342
C400
7d Monoc TTX

Figure 12. NF-H density in layer II/III of V1 for kittens in each condition.
**A**: Stereological measurement of NF-H density in V1 of normal kittens. **B**: Stereological measurement of NF-H density in V1 of kittens following a 7-day period of MD did not exhibit a change in density. **C**: Stereological measurement of NF-H density in V1 of kittens following a 10-day period of binocular retinal inactivation after a 7-day period of MD did not exhibit a change in density. **D**: Stereological measurement of NF-H density in V1 of kittens following a 10-day period of monocular retinal inactivation after a 7-day period of MD did not exhibit a change in density.